Ocean Engineering 250 (2022) 110958

Contents lists available at ScienceDirect

Ocean Engineering

journal homepage: www.elsevier.com/locate/oceaneng

Adaptation measures for seawalls to withstand sea-level rise

Dogan Kisacik [a,*], Gulizar Ozyurt Tarakcioglu [b], Lorenzo Cappietti [c]

[a] Department of Civil Engineering, Izmir Institute of Technology, Izmir, Turkey
[b] Department of Civil Engineering, Middle East Technical University, Ankara, Turkey
[c] LABIMA - Maritime Engineering Laboratory, Department of Civil and Environmental Engineering, University of Florence, Florance, Italy

ARTICLE INFO

Keywords:
Sea level rise
Coastal inundation
Wave overtopping
Vertical structure
Superstructure
Breaking waves
EurOtop manual
Stilling wave basin

ABSTRACT

Sea level rise necessitates adaptation measures for coastal protection structures like seawalls as changes in the design conditions will generate higher wave overtopping discharges and coastal flooding. Although increasing crest height is a common measure, the recreational function of urban seawalls limits the applicability. In this paper, performance on overtopping control of crest modifications such as storm walls, parapets, promenade, and stilling wave basin (SWB), are studied for simple and composite vertical seawalls. Two independent physical model studies from Turkey and Italy that cover a wide range of hydrodynamic conditions focusing on low relative freeboard are presented. Reduction factors that can be integrated into EurOtop prediction formulae (2018) are proposed within the experiment boundaries. The results show that a simple promenade, extending landward of a vertical seawall, provides very little reduction, whereas a seaward storm wall, under low freeboard conditions, is not effective as a similar storm wall once located on the landward edge of the promenade. Parapets decrease the overtopping further, however, the increase in relative freeboard influences the effect of parapets. Basin width and storm wall heights are important design parameters for SWB. Although the performance of different SWB configurations converges to lower reduction factors as the relative freeboard decreases, they perform better overall. Further analysis showed that the multiplication of the two individual reduction factors, one for the parapet effects and one for the promenade effects could provide an accurate representation of the composite reduction factor to determine the total effect. However, for complex geometries, it is seen that the composite reduction factors should reflect the interdependency of components when different elements with different mechanisms that change the overtopping discharge exist such as an overtopping bore on the promenade overtopping a storm wall. However, for developing future design guidelines, it is also important to consider the influence of individual components on the composite reduction factors such as the influence of storm wall height for a storm wall at the end of a promenade.

1. Introduction

Many low elevation coastal zones (LECZs) are more densely populated than the hinterland. They exhibit higher rates of population growth and urbanization and this trend is expected to continue (Neumann et al., 2015). At the same time, LECZs are vulnerable to coastal risks such as storm surges, overtopping, coastal flooding and their exposure will increase with foreseen sea-level rise related to climate change scenarios. Yearly mean sea-level rise in the Mediterranean area has been measured to be 1.3 mm/year, by analyzing tide gauge time series for the overall period from the last decades of the 19th century till 2012 (Zerbini et al., 2017). In the more recent decades, the rising rate has accelerated in coincidence with the rise of global temperatures and in the future global temperature scenarios, the sea-level rise projection is ranging from 75 to 190 cm for the period 1990–2100. These values will be even larger in subsiding coasts of the Mediterranean. The European Flood Directive 2007/60/EC points out the urgency of flood risk management plans while the Sendai Framework for Disaster Risk Reduction 2015–2030, endorsed by the UN General Assembly, highlights the need to adopt a multi-hazard approach for management across different sectors (The EU Floods, 2020 and, The United Nations Office for Disaster Risk Reduction, UNDRR). Identifying adaptive planning for LECZs coastal communities is thus mandatory, and in this perspective the development of innovative coastal protection systems, or adaptation measures of existing structures, is necessary.

Structures such as dikes and seawalls are common coastal protection

* Corresponding author.
E-mail addresses: dogankisacik@iyte.edu.tr (D. Kisacik), gulizar@metu.edu.tr (G.O. Tarakcioglu), lorenzo.cappietti@unifi.it (L. Cappietti).

https://doi.org/10.1016/j.oceaneng.2022.110958
Received 1 October 2020; Received in revised form 24 February 2022; Accepted 25 February 2022
Available online 17 March 2022

alternatives utilized to reduce these risks. The design and performance of these structures depend on several conditions including water levels, waves, surges, tides. For many of the present coastal structures, a change in the design conditions is reflected in the performance in terms of higher overtopping discharges, coastal flooding, and damages to the economy and infrastructure. Therefore, an adaptation of the existing structures is to be required for these new hydrodynamic conditions. A common measure to reduce the average overtopping discharge is to increase the crest height of the structures based on the new design conditions. However, there are desirable limits to the crest heights of these structures since many coastal areas are widely utilized for recreational purposes that require ease of access to the sea and the preservation of the sea scenery. Such restriction could be overcome by building low storm walls, parapets, promenades (i.e. increasing the area between the coastal structures and urban area), or an assembly of them for creating a superstructure like a stilling wave basin (Fig. 1). To determine the performance of these modification measures to reduce the overtopping discharges, thus attenuating the foreseen impacts in the climate change scenarios is one of the present challenges for the coastal engineering research community.

The present knowledge on some alternatives of crest modifications to reduce overtopping on sloping coastal structures such as dikes is extensive. Prediction formulas and design requirements are presented in EurOtop (2018) in detail. On the other hand, a similar level of knowledge is not available for the modification of vertical structures such as urban seawalls fronted by shallow waters. The location of urban seawalls exposes them to breaking or broken wave conditions that mostly generate impulsive overtopping conditions for which limited knowledge exists for crest modifications as well. Moreover, the effectiveness of superstructures composed by an assembly of the different components (e.g. storm walls, parapets, SWB) still needs to be assessed for the case of non-pulsating wave conditions. This paper presents and discusses the reduction of overtopping by crest modification of vertical seawalls based on the results of two independent experimental studies in Turkey and Italy.

The first study focused on the reduction of overtopping over a simple vertical wall with a promenade based on characteristics of the urban shoreline of Izmir, Turkey. Kisacik et al. (2019) presented the performance of a stilling wave basin design (SWB) on the referenced structure by physical modelling, testing a wide range of hydrodynamic conditions including the local conditions for the design. The majority of the tested conditions are impulsive conditions. They discussed the optimization of such a design and showed the applicability for existing urban seawalls, to adapt these structures for higher overtopping values. However, SWB is a combination of different crest modification structures and might not apply to many urban areas with vertical seawalls. Therefore, in this paper, different crest modifications (which can also be components of SWB) are tested and analyzed for the same reference vertical wall under a wide range of hydrodynamic conditions building on the initial SWB assessment of Kisacik et al. (2019). The results are expected to provide an initial assessment of the influence of such superstructures under impulsive conditions on the mean overtopping discharge as relative freeboard condition decreases with sea-level rise.

The second study assessed similar crest modifications and SWB for a vertical wall breakwater structure with a foreshore of 1:7 (Crema et al., 2009). The vertical wall with a rubble-mound base is a composite vertical structure that was tested under a variety of hydrodynamic conditions. Contrary to the simple vertical seawall of the first study, the overtopping for this vertical wall was mostly non-impulsive. These tests enhanced the discussion on the effectiveness of SWB and similar crest modifications for a wider overtopping regime. The very steep foreshore and the rubble-mound base that characterizes this second experimental campaign gives the opportunity of expanding the analysis toward more general conditions thus widening the impacts of the present study. At the same time, it is worth pointing out that the presence of very steep foreshore and the rubble-mound base required further discussions on the selection of the overtopping formulae presented in EurOtop (2018) for a composite vertical wall structure.

These combined results of the two studies show the effectiveness of different modification measures such as including a storm wall, parapet, promenade, and SWB in reducing the overtopping for a variety of hydrodynamic conditions and geometries by providing reduction factors based on physical tests. The selected measures also consider the unique limitations such as demand for low crest heights and availability of space for certain coastal areas used for recreation or urbanization. Therefore, a more comprehensive assessment of reducing overtopping in vertical seawalls by crest modification is aimed to be presented in this paper built on the discussion of Kisacik et al. (2019). The available overtopping prediction formulas for different superstructures are summarized in the literature review section. In methodology, the experimental campaigns of the two studies are presented. The overtopping results and the calculated reduction factors for each superstructure are provided in the results section. Next, the influence of each crest modification as well as analysis of components of SWB configurations are discussed and these discussions points are summarized in the conclusion.

2. Literature review

A variety of superstructures are designed to modify the crest of coastal protection structures to control the overtopping. Contrary to sloping structures, waves at vertical walls may push the water vertically which may partly overtop over the crest and partly fall back into the water. The objective of such crest modifications is to return the uprushing wave seawards, decreasing the overtopping. These (Fig. 1) include:

a) Promenade with slope
b) Storm wall
c) Parapet with different angles

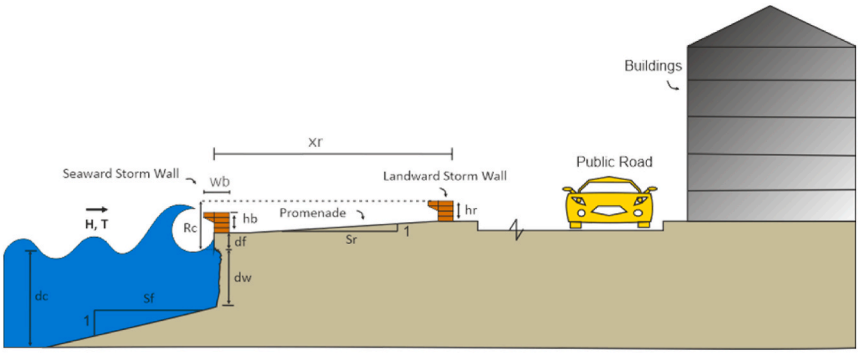

Fig. 1. Different superstructure elements possible for an urban vertical seawall.

d) And the combination of all above like SWB

There are no real guidelines on how such superstructures should geometrically be designed, but the size and shape of the structure have a large influence on the effect of wave overtopping. This influence on wave overtopping is considered by introducing reduction factors in the overtopping equations. The reduction factors are determined from experimental investigations by comparing the overtopping performance of a reference case such as a simple vertical wall, to the cases with crest modifications. A reduction factor smaller than one, describes less wave overtopping due to the crest modification.

There are many approaches to determine the overtopping discharge for vertical walls in the literature. EurOtop (2018) is a widely accepted guideline that provides the latest methods and techniques to determine the overtopping discharge values for most of the coastal structures including vertical walls tested in this study. Throughout this study, the formulations presented in EurOtop (2018) are used to predict and determine the reduction factors of different crest modifications. A review of the existing knowledge on the promenade (or boulevard) with slope, storm wall, parapet with different angles (i.e., bullnose), and SWB is provided in this section.

a) Promenade (or boulevard) with slope

The (quasi) horizontal part at the crest that is usually above the still water level is called the promenade (Fig. 1). It contains a gentle slope of 1%–2% to stimulate draining from rainfall and overtopped water towards the sea (Van Doorslaer et al., 2015). As a rule of thumb, the hazard effect of overtopping discharge at a point x meters away from the seawall crest will be reduced by a factor of x (over a range of 5–25 m, EurOtop, 2018). Therefore, the longer the promenade length, the less overtopping occurs at the end of the promenade (Van Doorslaer et al., 2010). In EurOtop (2018), a reduction factor for a promenade on a dike is proposed (Eq. (1)).

$$\gamma_{prom} = 1 - 0.47\frac{X_r}{L_{m-1,0}} \tag{1}$$

For $\frac{X_r}{L_{m-1,0}} = 0.05 - 0.5$, this equation shows that the reduction depends on the dimensionless promenade width as also stated by Tuan (2013). However, no equation is presented for the case of a promenade on a vertical seawall.

b) Storm wall

It is very practical to increase the crest height of a vertical wall by building a storm wall on the sea side of the structure. Similarly, a landward storm wall would modify the crest of a seawall by introducing a promenade and a storm wall as a combined superstructure as also shown in Fig. 1. For the case of the seaward storm wall, the prediction formulas for the simple seawall are utilized but the crest height includes the height of the seaward storm wall (Fig. 1). However, no such recommendation exists in EurOtop (2018), since the existence of a landward storm wall includes a promenade component making the crest modification a complex superstructure.

The research on storm walls on dikes (Tuan (2013), Van Doorslaer et al. (2010), Van Doorslaer and De Rouck (2010), Van Doorslaer et al. (2015), and Zanuttigh and Formentin (2018)) show that reduction factor for seaward storm wall exponentially varies with the wall height. However, two different conclusions exist for the combined superstructure of the storm wall at the end of a promenade on a dike. Tuan (2013) described a new overall wall influence factor γ_{prom_v} as the product of the reduction effect of promenade width in front of a storm wall of constant height and the height of this storm wall itself. Therefore, the reduction factor γ_{prom_v} is determined as (Eq. (2));

$$\gamma_{prom\_v} = \gamma_v \cdot \gamma_{prom} \tag{2}$$

where γ_v and γ_{prom} are influence factors of wall height (h_b) and wall promenade, respectively. For the influence factor γ_v (Eq. (3)), part of the wall height is included in the crest freeboard (R_c) according to the behavior of waves on the slope (Tuan, 2013).

$$\gamma_v = \frac{1}{1 + 1.60\frac{h_b}{R_c}\cdot\frac{1}{\zeta_{0m}}} \tag{3}$$

where ζ_{0m} is the Iribarren number determined according to the spectral period $T_{m\text{-}1,0}$. The influence of promenade (γ_{prom}) is found to be best correlated with the dimensionless promenade width, $\frac{X_r}{H_{m0}}$ (Tuan, 2013) where X_r is the promenade width (Eq. (4)).

$$\gamma_{prom} = \frac{1}{1 + \frac{1}{8}\frac{X_r}{H_{m0}}\frac{1}{\zeta_{0m}}} \tag{4}$$

The results for the wall promenade influence factor are based on a combined geometry of constant wall height and a promenade, not a simple promenade with a certain width (Tuan, 2013). Although the scatter of data points to a dependency on wall height for the wall promenade factor, Tuan (2013) concluded that the dependency is rather weak and might be practically unimportant. Still, he discussed the necessity of further work to clarify this mutual dependency. The results showed that the reduction in wave overtopping due to the wall promenade was rather low compared to the wall height effect. This is probably due to a relatively narrow promenade considered in the study. Experimental data by Van Doorslaer et al. (2010) with narrow berms shows a similar result (Tuan, 2013).

On the other hand, Van Doorslaer et al. (2015) showed that the product of individual reduction factors of storm wall height and promenade leads to an underestimation of the reductive effect of the actual combined superstructure as shown in Eq. (5).

$$\gamma_{prom\_v} = 0.87\gamma_v\,\gamma_{prom} \tag{5}$$

where γ_{prom} is calculated using Eq. (4) and γ_v is defined as follows (for smooth dike slopes) under non-breaking waves:

$$\gamma_v = \exp\left(-0.56\frac{h_b}{R_c}\right) \tag{6}$$

This result indicates that individual reduction factors can not simply be multiplied to account for the combined effect (Van Doorslaer et al., 2015) since the physical process of waves hitting a wall is different when a promenade is present in front of the storm wall.

Further experiments were performed by Zanuttigh and Formentin (2018) to analyze dikes with a finite horizontal crest width and an inshore crown wall (similar to the case of storm wall at the end of a promenade), with and without a bullnose, subjected to both breaking and non-breaking wave conditions. A modification of the reduction factor of Van Doorslaer et al. (2015) by introducing the breaker parameter $(\xi_{m-1,0})$ for breaking wave conditions was proposed:

$${\gamma_{prom\_v}}^* = \frac{\gamma_{prom\_v}}{\tanh\left(\xi_{m-1,0}\right)} \tag{7}$$

Further research showed that for the case of a storm wall at the end of a promenade on a dike, the important parameters that affect the reduction factor are promenade width, wall height, and breaker parameter (Zanuttigh Formentin, 2018).

It might be possible to extend this discussion for vertical seawalls, as similar physical process changes were observed along the promenade for the overtopping volume during our tests (as discussed in Kisacik et al. (2019)). Therefore, the reduction factor regarding such a superstructure might be independent of the main structure type (sloping or vertical structure). We aim to provide some insight into this possibility assuming

that the influence of the breaker parameter for sloping structures could be reflected as impulsiveness for overtopping over a vertical wall.

c) Parapet with different angles (Bullnose)

Parapets are seaward extensions that are generally designed as an overhanging cantilever on a storm wall with different nose angles. Recurves are curved parapets or walls with fully curved seaward faces. In presence of a parapet, waves are not only projected upward but also back to the sea (Van Doorslaer and De Rouck, 2010). This behavior reduces the overtopping volume more significantly than a simple increase in storm wall height (Kortenhaus et al., 2002).

The principle of a parapet has already been introduced to reduce wave overtopping at vertical seawalls (Goda, 1985; Franco et al., 1994), and a few tests have been executed by Den Heijer (1998) with a fixed parapet at a sloping seawall with a berm. In the previous papers, a non-variable reduction factor $\gamma_p = 0.7$ has been proposed (as cited in Van Doorslaer and De Rouck, 2010). In EurOtop (2018), the influence of parapets on vertical seawalls is presented in detail. There are three regimes of effectiveness where no effect, moderate effect, and significant effect can be observed based on relative freeboard (which includes the additional crest height due to parapet). Accordingly, the following equations (Eq. (8)) are provided to determine the reduction factor for parapet on seawalls (EurOtop, 2018).

$$\gamma = 1.0 for \frac{R_c}{H_{m0}} \leq 0.5$$

$$\gamma = 1.3 - 0.6\frac{R_c}{H_{m0}} for 0.5 < \frac{R_c}{H_{m0}} \leq 1.0 \tag{8}$$

$$\gamma = 0.7 for \frac{R_c}{H_{m0}} > 1.0$$

Kortenhaus et al. (2002) report on a series of tests with various nose angles and length of the inclined section of the parapet. The parapet worked out well under conditions where the relative crest freeboard is high, $R_c/H_s > 1.5$ (Kortenhaus et al., 2002). They quantified the effectiveness of the recurve/parapet in reducing overtopping by the k-factor (k_{bn}) defined as in Kortenhaus et al. (2002) and presented in EurOtop (2018):

$$k_{bn} = \frac{q_{with\_bullnose}}{q_{without\_bullnose}} \tag{9}$$

However, high scatter was observed in the lowest k regime. Therefore, Pearson et al. (2004) extended the study to focus on this regime of the largest reduction factors. In this region, they claim to see a clear dependency of the wave period on the overtopping discharges. The dependency of overtopping on the angle of the parapet, height of the parapet, the width of the parapet, relative freeboard, and ratio of crest height to the water depth at the toe of the structure are summarized and provided in EurOtop (2018) as a flowchart. It is suggested that designing for $k_{bn} < 0.05$ is impractical given the level of scattering in the original data and uncertainties related to physical mechanisms. If such large (or larger) reductions are required, a detailed physical model study should be considered.

Martinelli et al. (2018) also measured wave overtopping at recurved parapets of a simple vertical breakwater using four different parapet angles of 0°,45°,60° and 90° and extensions under non-breaking wave forces. They observed that the measured overtopping rate appeared to be well predicted by the formula and flowcharts proposed by EurOtop (2018). While EurOtop (2018) provides guidance on the reduction factor for parapets/bullnose on a vertical wall, the location of the parapet is always on the seaside. and there is no guidance for. While the case of a parapet on a landward storm wall at the end of a promenade was studied for dikes by Van Doorslaer et al. (2015) and Zanuttigh and Formentin (2018), there is no such guidance for the vertical walls. The results for dikes showed that the reduction factor of a storm wall with a parapet at the end of a promenade cannot be determined by multiplying the individual reduction factors of the storm wall, promenade, and the parapet. For dikes, the reduction factor for the combined superstructure is less efficient than the product of individual factors (Van Doorslaer et al., 2015). Therefore, in this study, we included tests for parapets on the seaward storm wall (as in the literature) but also for parapets on the landward storm wall at the end of a promenade.

d) Stilling Wave Basin

EurOtop (2018) defines Stilling Wave Basin (SWB) as an area designed in front of the crest or capping wall, where a part of the up-rushing wave may remain without overtopping. The SWB is made up of a partially permeable seaward storm wall, a sloping promenade (basin), and a landward storm wall. The seaward storm wall may consist of a double row of shifted storm walls or a single storm wall with some gaps to allow drainage of the water in the basin. Landward and seaward storm walls may have bullnose geometries of different angles (Geeraerts et al., 2006; Van Doorslaer et al., 2009).

This crest design is based on the principle of energy dissipation. The incoming wave dissipates most of its energy by hitting the seaward storm wall and through the basin before it reaches the landward storm wall. Consequently, the landward wall is overtopped less in comparison with an unmodified crest, even though the crest height has not been increased (Van Doorslaer et al., 2015). A detailed literature review of SWB as a superstructure is presented in Kisacik et al. (2019). In summary, effectiveness for SWB depends on several factors such as the height of storm walls, number of rows, and blocking coefficient.

For SWB on sloping structures, EurOtop (2108) proposes a reduction factor of 0.45. Moreover, Cappietti and Aminti (2012) proved that building SWB in front of wave walls of rouble-mound breakwaters can reduce the overtopping discharge up to a factor of 2. Furthermore, they proved that although the same reduction can be achieved by increasing the height of the wave wall, the use of SWB in conjunction with a lower wave wall would still be a better alternative in terms of a higher reduction of the maximum wave-by-wave overtopping volumes. However, there is no general recommendation for SWB on vertical structures. Kisacik et al. (2019) derived a set of reduction factor equations for a specific SWB geometry on the vertical structure under impulsive conditions. The proposed reduction factors (Eqs. (10) and (11)) are based on freeboard conditions.

Low freeboard condition (Greenwater type) $(0.1 < R_c/H_{m0} < 1.35)$

$$\gamma_{SWB\_low} = -0.0615\frac{R_c}{H_{m0}} + 0.577, \qquad 0.708 \leq \frac{R_c}{H_{m0}} < 1.35 \tag{10}$$

High freeboard condition (splash/spray type) $(R_c/H_{m0} \geq 1.35)$

$$\gamma_{SWB\_high} = -0.3812\frac{R_c}{H_{m0}} + 0.828, 1.35 \leq \frac{R_c}{H_{m0}} \leq 2.09 \tag{11}$$

It is observed that the reduction factor varies in the range of $0.39 \leq \gamma_{SWB} \leq 0.62$ and $0.05 \leq \gamma_{SWB} \leq 0.31$, for low and high freeboard conditions, respectively. These reduction factors can be integrated into the EurOtop (2018) prediction equations of vertical structures with foreshore influence and impulsive conditions. However, the efficiency of SWB highly depends on its geometry and hydrodynamic conditions, therefore physical model tests should be performed for any new SWB design.

3. Experimental set-up

Two vertical seawalls in Turkey and Italy were tested to determine the overtopping reduction factors of different superstructures. The test setups, hydrodynamic conditions, and the equipment used are presented in this section.

3.1. Experimental setup of the simple urban seawall (Turkey)

The physical model tests were carried out in the wave flume of Coastal and Harbour Engineering Laboratory, Department of Civil Engineering of Middle East Technical University (METU, Turkey). The wave flume is 26 m in length, 6 m in width, and 1.0 m in depth. An inner channel with glass side walls (18.00 m in length, 1.50 m in width) is constructed in the wave flume to reduce the size of the cross-section and the effects of reflection occurring due to concrete sidewalls. A slope of plastic wire scrubbers acting as wave absorbers is installed at the end of the flume as a passive absorption system. Irregular waves are generated by a piston-type wave maker which is placed at the other end of the wave flume (Fig. 2). Each time series of the experiments contained 500 irregular waves with the Bretschneider spectrum.

The experiments were performed for: a) the present seawall, b) without a scaled model (to determine undisturbed wave conditions) and c) a variety of superstructures. The cross-section of the present seawall and the foreshore slope ($S_f = 1/20$) was determined by considering seven cross-section measurements of the Kordon seawall and promenade in Izmir, Turkey. The initial hydrodynamic conditions tested in this study were based on hydraulic boundary conditions for Kordon seawall however additional changes in the water depth and wave heights provided a total of 26 different hydrodynamic conditions (Table 1). The changes in the water depth influenced the crest height and freeboard of each superstructure accordingly. This approach provided a larger dataset to determine the influence of superstructure for a variety of crest heights without changing the structure dimensions.

The standard 3-gauge procedure of Mansard and Funke (1980) was applied to wave gauges 8, 9, and 10 to determine the incident significant wave heights and periods in front of the structure using the results of the cases without the scaled model. Overtopping water was collected in a tank behind the superstructures and the mean wave overtopping discharge was calculated at the end of each test. As these experiments are the extension of a previous campaign, the model is set up and more information is presented in Kisacik et al. (2019).

Nine superstructures are tested as presented in Fig. 3 (i-ix). The Froude scale was set as 1:16 after considering the limits of water depth and wave maker capacity. Case i presents a sloping promenade on top of a vertical seawall which has a height of 0.21 m ($d_w + d_f$) in model scale. Here the slope of the promenade is selected as 2% (S_r) and the width is $x_r = 0.5$ m (8 m in prototype) reflecting the local conditions of Izmir, Turkey. In this case, the crest height is taken from the landward end of the promenade. The promenade dimensions were kept constant for all the superstructures tested in the study. Different combinations of storm walls on seaward and landward are tested with the promenade configuration. The heights ($h_b = h_r = 0.04$ m) and widths ($w_b = 0.03$ m) of these storm walls are kept constant for all the setups. When bullnose/parapet is included on the storm walls, the total height of the superstructure is kept the same as the case of storm walls without a parapet. This setup enabled us to determine the influence of the parapet independent of any change in overall crest height. Case ii is the storm wall and parapet combination in front of a promenade which provides a higher crest height than case i. The crest height of this case is taken from the top of the parapet but since the overtopped water was collected after the promenade, the overtopping volume is expected to be influenced by the promenade as well. Case iii is a storm wall at the end of a promenade combination, therefore overtopping is expected to be influenced by the promenade first and then the storm wall. Case iv is a modified version of case iii with a parapet on the storm wall. Case v is a double row SWB on seaward that also integrates the promenade and the continuous landward storm wall. The distance between the double rows of seaward storm walls (Δx) is 0.04 and the blockage coefficient (C_b) for all SWB cases is decided as 66.7% based on the optimization study presented in Kisacik et al. (2019). The overall crest height of this superstructure is the same as in previous cases. Case vi is the modified version of case v with a parapet on the landward storm wall while Case vii is the modified version of Case v with a parapet on the first row of the seaward storm wall. Case viii is the combination of cases vi and vii, keeping the crest height constant. Case ix is a single row SWB with a continuous storm wall at the end of a promenade where both storm walls have parapets.

For those cases with a parapet, parapet angle (β) is selected as 30° following the recommendation of Van Doorslaer et al. (2015). The other parameters for the parapet are set as $h_n = 2cm$, $h_b = 4cm$, $w_b = 3cm$, $w_{\_parapet} = 5cm$ and $\lambda = 0.5$ in model scale (Fig. 4).

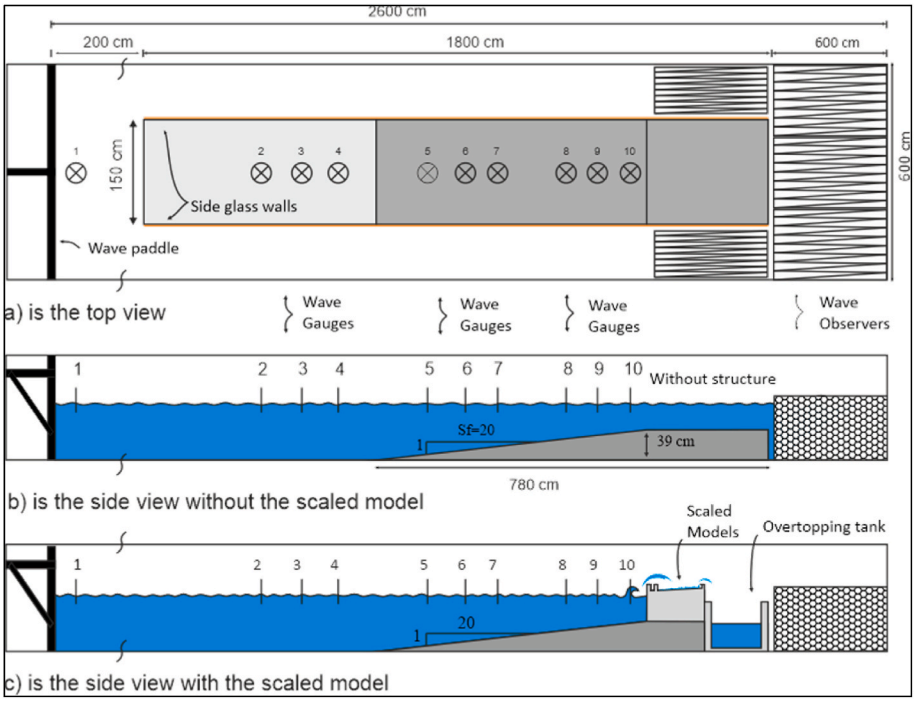

Fig. 2. Flume model set-up, used for irregular wave tests for urban seawall (Turkey).

Table 1
Test parameter matrix for superstructures – urban seawall (Turkey).

Test #	d_c (m)	d_w (m)	d_f (m)	H_{m0} (m)	$T_{m-1,0}$ (s)	Crest Freeboard (R_c)								
						i (m)	*ii* (m)	*iii* (m)	*iv* (m)	*v* (m)	*vi* (m)	*vii* (m)	*viii* (m)	*ix* (m)
1	0.600	0.200	0.010	0.081	1.26	0.023	0.050	0.063	0.063	0.063	0.063	0.063	0.063	0.063
2	0.581	0.181	0.029	0.075	1.26	0.042	0.069	0.082	0.082	0.082	0.082	0.082	0.082	0.082
3	0.563	0.163	0.047	0.069	1.22	0.060	0.087	0.100	0.100	0.100	0.100	0.100	0.100	0.100
4	0.544	0.144	0.066	0.067	1.26	0.079	0.106	0.119	0.119	0.119	0.119	0.119	0.119	0.119
5	0.600	0.200	0.010	0.088	1.37	0.023	0.050	0.063	0.063	0.063	0.063	0.063	0.063	0.063
6	0.581	0.181	0.029	0.085	1.50	0.042	0.069	0.082	0.082	0.082	0.082	0.082	0.082	0.082
7	0.563	0.163	0.047	0.083	1.33	0.060	0.087	0.100	0.100	0.100	0.100	0.100	0.100	0.100
8	0.544	0.144	0.066	0.076	1.45	0.079	0.106	0.119	0.119	0.119	0.119	0.119	0.119	0.119
9	0.525	0.125	0.085	0.071	1.37	0.098	0.125	0.138	0.138	0.138	0.138	0.138	0.138	0.138
10	0.581	0.181	0.029	0.104	1.61	0.041	0.069	0.081	0.081	0.081	0.081	0.081	0.081	0.081
11	0.563	0.163	0.048	0.092	1.61	0.060	0.088	0.100	0.100	0.100	0.100	0.100	0.100	0.100
12	0.544	0.144	0.066	0.084	1.61	0.079	0.106	0.119	0.119	0.119	0.119	0.119	0.119	0.119
13	0.525	0.125	0.085	0.076	1.61	0.098	0.125	0.138	0.138	0.138	0.138	0.138	0.138	0.138
14	0.506	0.106	0.104	0.075	1.72	0.116	0.144	0.156	0.156	0.156	0.156	0.156	0.156	0.156
15	0.563	0.163	0.047	0.094	1.72	0.060	0.087	0.100	0.100	0.100	0.100	0.100	0.100	0.100
16	0.544	0.144	0.066	0.090	1.66	0.079	0.106	0.119	0.119	0.119	0.119	0.119	0.119	0.119
17	0.525	0.125	0.085	0.084	1.66	0.098	0.125	0.138	0.138	0.138	0.138	0.138	0.138	0.138
18	0.506	0.106	0.104	0.080	1.66	0.117	0.144	0.157	0.157	0.157	0.157	0.157	0.157	0.157
19	0.563	0.163	0.048	0.105	1.72	0.060	0.088	0.100	0.100	0.100	0.100	0.100	0.100	0.100
20	0.544	0.144	0.066	0.098	1.79	0.079	0.106	0.119	0.119	0.119	0.119	0.119	0.119	0.119
21	0.525	0.125	0.085	0.092	1.79	0.098	0.125	0.138	0.138	0.138	0.138	0.138	0.138	0.138
22	0.506	0.106	0.104	0.086	1.79	0.116	0.144	0.156	0.156	0.156	0.156	0.156	0.156	0.156
23	0.563	0.163	0.048	0.114	2.02	0.060	0.088	0.100	0.100	0.100	0.100	0.100	0.100	0.100
24	0.544	0.144	0.066	0.108	2.02	0.079	0.106	0.119	0.119	0.119	0.119	0.119	0.119	0.119
25	0.525	0.125	0.085	0.103	2.02	0.098	0.125	0.138	0.138	0.138	0.138	0.138	0.138	0.138
26	0.506	0.106	0.104	0.095	2.02	0.116	0.144	0.156	0.156	0.156	0.156	0.156	0.156	0.156

3.2. Experimental setup of the composite vertical seawall (Italy)

The experimental tests for the composite vertical seawall have been conducted in the wave-current flume of LABIMA, the Maritime Engineering Laboratory of the Civil Engineering Department of Florence University (Italy). The wave flume is 4.7 m long, 0.8 m in height, and 0.8 m wide, and it is equipped with a piston-type wave maker. The models were located 4.058 m away from the wave paddle on a uniform foreshore slope, 1/7. The vertical wall is located on a submerged rubble mound berm breakwater in natural rocks of 3.9–7.8 g. The berm is 11.2 cm wide and placed at a depth between 24.3 cm and 33.3 cm from the bottom of the flume. The seaward slope of the berm is 1:1.5. The model setup and the instrumentation are presented in Fig. 5.

The model was instrumented with five resistive type wave gauges, an overtopping tank collector, and a video camera that was used to capture the wave overtopping process. Two wave gauges in front of the wave maker controlled the wave generation. Three wave gauges in front of the breakwater model were used to measure the reflected and incident waves.

The test was performed under 9 different wave conditions characterized by a JONSWAP spectrum with peak enhancement factor 3.3 (Table 3). As the wave parameters were measured with the scaled model present in the flume, wave reflection affected the measurement of incident wave parameters. Therefore, only the fragment of the test during which the re-reflection had not reached the breakwater model was used for the data analysis (120 s of wave generation). Four different time series have been reproduced in the flume for a given wave attack characterized by a given frequency spectrum to increase the length of each overtopping test. The 2-min long interval, almost free from the re-reflection of the four-wave attacks, has been merged to obtain 8-min long time series which has been used for the overtopping analysis (i.e. about 300–500 waves for the varying wave periods).

Three different crest modifications for the composite vertical seawall (wall height = $d_w + d_f = 0.205$ m) were tested (Crema et al., 2009). The Froude model scale was set as 1:80 after considering the limits of water depth in the flume and wave maker capacity to ensure the correct reproduction of all wave processes. These models are configured to assess the overtopping reduction factor of the pattern of the gaps in the storm walls, the horizontal width of the promenade (x_r), the height and width of the landward storm wall (h_r, w_r), and the height and width of the seaward storm wall (h_b, w_b). For all the configurations (Fig. 6), the crest height of the superstructure is kept constant to ensure that the reduction in overtopping is independent of the crest height and depends only on the different configurations of these superstructures.

C5 is a configuration of a storm wall at the end of a narrow promenade ($X_r/2 = 0.125$ m). C8 is a configuration of a storm wall at the end of a wider promenade ($X_r = 0.25$ m). The landward storm wall height ($h_r = 0.075$ m) and width ($w_r = 0.025$ m) are constant for all configurations. C6 is an SWB configuration with a single row seaward storm wall with holes on it (11 holes with 1 cm diameters) which corresponds to a blocking coefficient (C_b) of 95.1% (Fig. 7 a,b). The height and width of the seaward row are smaller ($h_b = 0.022$, $w_b = 0.021$) than the landward storm wall and the basin which can be considered as a promenade is narrow ($X_r/2 = 0.125$ m).

The overtopped water was collected in an overtopping tank by a chute connecting the landward storm wall to the overtopping tank. Wave by wave overtopping volumes has been measured by using a load cell in the overtopping tank(Crema et al., 2009)(Fig. 7c). Then, mean overtopping discharges are calculated from individual overtopping volumes.

4. Results

The overtopping discharge values for each configuration measured during the physical model tests for the two seawalls are presented as graphs of relative overtopping discharge vs relative freeboard and reduction factor vs relative freeboard. The first part of this section discusses the overtopping behavior of the simple and composite vertical walls and the application of EurOtop's (2018) prediction formulas. In the second part, the effectiveness of different superstructures with respect to each other is compared using reduction factors based on the reference trendlines.

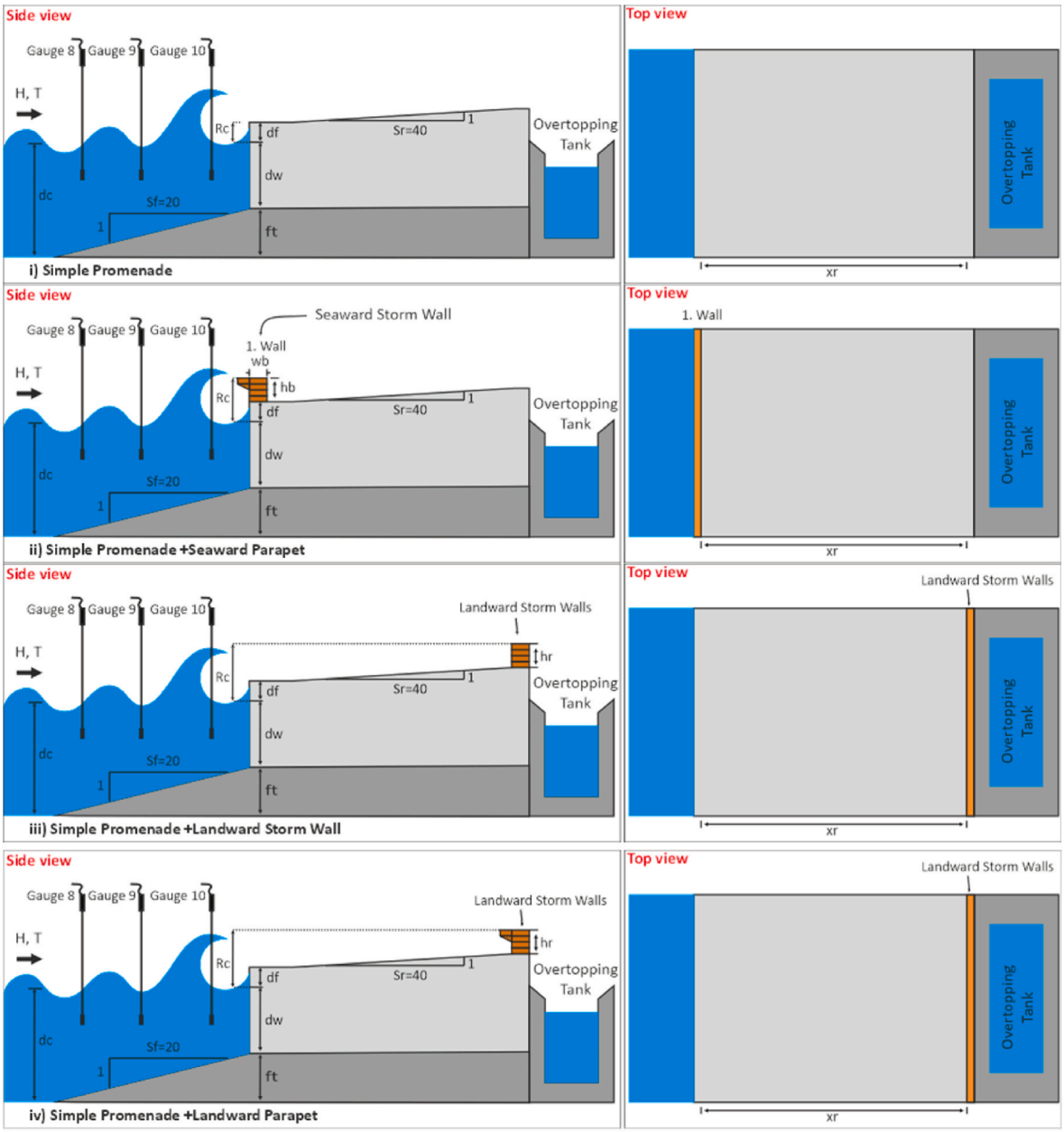

Fig. 3. Scaled models of the 9 different super structures tested in the present study (urban seawall, Turkey).

4.1. Overtopping discharge rates of crest modifications and reference cases

The influence of superstructures can be quantified by comparing the overtopping values to the values of a reference case that is the conventional vertical wall geometry under the same foreshore and hydrodynamic conditions. These reference curves are determined from the trendlines of the overtopping values using the prediction formulae in EurOtop (2018). Therefore, the selection of the prediction formulae and their applicability to the reference cases is presented in this section. The reference cases in this study are the two tested vertical seawalls (including the foreshore conditions) without crest modifications.

The first reference case is the simple seawall setup based on the Kordon seawall of Izmir, Turkey. As presented in Kisacik et al. (2019), the seawall has an influencing foreshore with a slope of 1/20. This reference case was tested under the same hydrodynamic conditions presented in this study. All the waves break at the structure generating impulsive overtopping conditions (i.e. $\frac{h^2}{H_{m0}.L_{m-1,0}} \leq 0.23$). In Kisacik et al. (2019), these measured values were compared to the computed values based on the prediction formulas of EurOtop (2018). The results showed that one standard deviation increased version of the prediction formula for simple vertical walls under impulsive overtopping conditions (Eqs. (12) and (13)), representing the trendline of the measurements accurately.

$$\frac{q}{\sqrt{g.H_{m0}^3}} = 0.0155\left(\frac{H_{m0}}{hs_{m-1,0}}\right)^{0.5}.exp\left[-2.2\frac{R_c}{H_{m0}}\right] 0.1 < R_c \Big/ H_{m0} < 1.35 \tag{12}$$

$$\frac{q}{\sqrt{g.H_{m0}^3}} = 0.0020\left(\frac{H_{m0}}{hs_{m-1,0}}\right)^{0.5}\left[\frac{R_c}{H_{m0}}\right]^{-3} R_c \Big/ H_{m0} \geq 1.35 \tag{13}$$

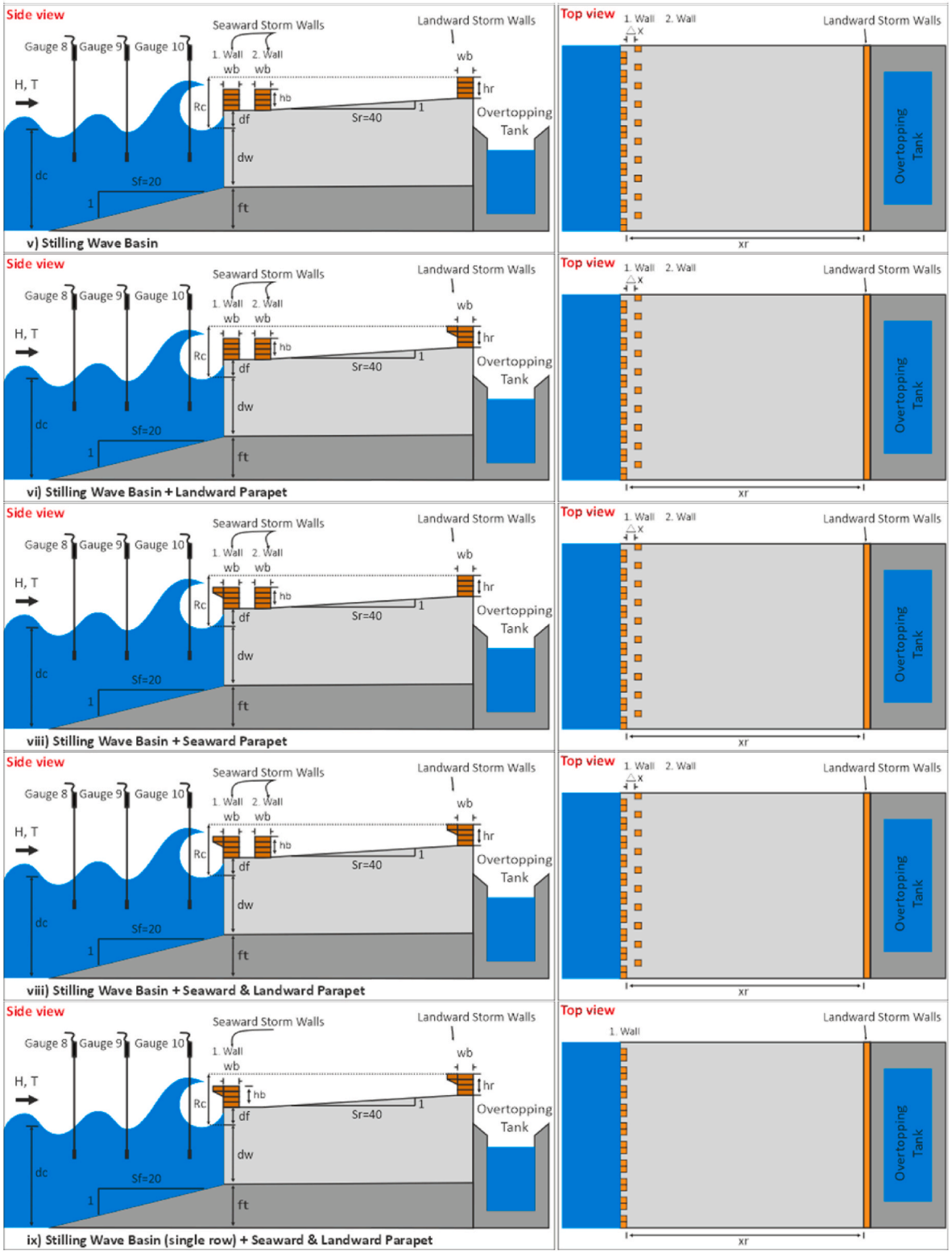

Fig. 3. (*continued*).

where q is the wave overtopping discharge; R_c is the crest freeboard; H_{m0} is the spectral significant wave height; $s_{m-1,0}$ is the (fictitious) mean wave steepness, $L_{m-1,0}$ is deep water wave length and h is water depth in front of the toe of the structure. As a result, the reference trendline for the experiments of the simple vertical seawall is only based on one formula with respectively low and high freeboard conditions which is the actual prediction formula presented as Eq. 7.9 and 7.10 in EurOtop (2018). Therefore in the figures and discussions, this reference trendline will be denoted as the EurOtop (2018) reference trendline.

The second reference case is the composite vertical structure with a mound and a very steep foreshore (1:7), tested by Crema et al. (2009). Although the cross-section without crest modifications was not tested experimentally, the one sigma approach of the prediction formulae is used to predict the reference trendline and to maintain comparability

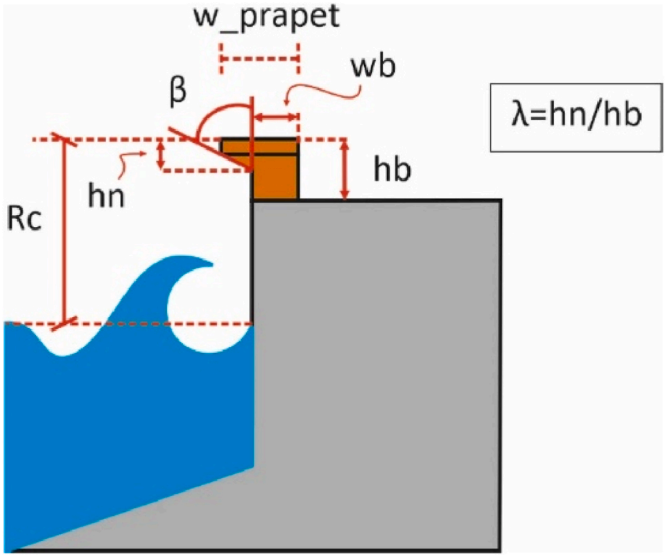

Fig. 4. Parapet parameters used in the tests (simple vertical seawall).

between Izmir and Italy experiments. For the composite vertical structures, EurOtop (2018) proposes to use modified versions of prediction formulas derived for the simple vertical seawall. The procedure to determine the prediction formula requires analyzing the influence of the foreshore, the influence of the mound, and the impulsiveness of the waves. Since the foreshore of the structure is very steep (1:7), the foreshore can also be assumed as part of the structure extending the slope of the original mound, following the recommendation of EurOtop (2018). Therefore, the toe of the structure could be defined as the base of the steep slope which is included as part of the structure whereas the mound depth is the water depth over the rubble mound toe in front of the vertical wall (Fig. 9a). Thus, the influence of the foreshore is analyzed for the hydrodynamic conditions tested using the wave gauge data on the horizontal bed and along the foreshore.

Two of the test conditions (I6 and I21) are not influenced by the foreshore, therefore following steep foreshore recommendation, the foreshore part is assumed to be part of the whole structure and consequently, the foreshore of these cases is the flume bed. When the foreshore is horizontal in front of a composite vertical seawall and it does not influence the wave conditions, EurOtop (2018) states that the composite vertical structure behaves like a simple vertical seawall. Therefore, prediction formula for a simple seawall with no influencing foreshore increased by one sigma (Eq. (14), for assessment approach) is used to determine the overtopping values for conditions I6 and I21 as a reference condition

Table 3
Test parameter matrix for composite vertical seawall (Italy).

Test#	d_c (m)	d_w (m)	H_{m0} (m)	$T_{m-1,0}$ (s)	R_c (m)
I3	0.52	0.187	0.054	1.37	0.094
I6	0.52	0.187	0.060	1.14	0.094
I7	0.52	0.187	0.069	1.23	0.094
I8	0.52	0.187	0.071	1.24	0.094
I9	0.52	0.187	0.077	1.39	0.094
I10	0.52	0.187	0.085	1.60	0.094
I11	0.52	0.187	0.066	1.77	0.094
I21	0.52	0.187	0.055	1.14	0.094
I22	0.52	0.187	0.060	1.25	0.094

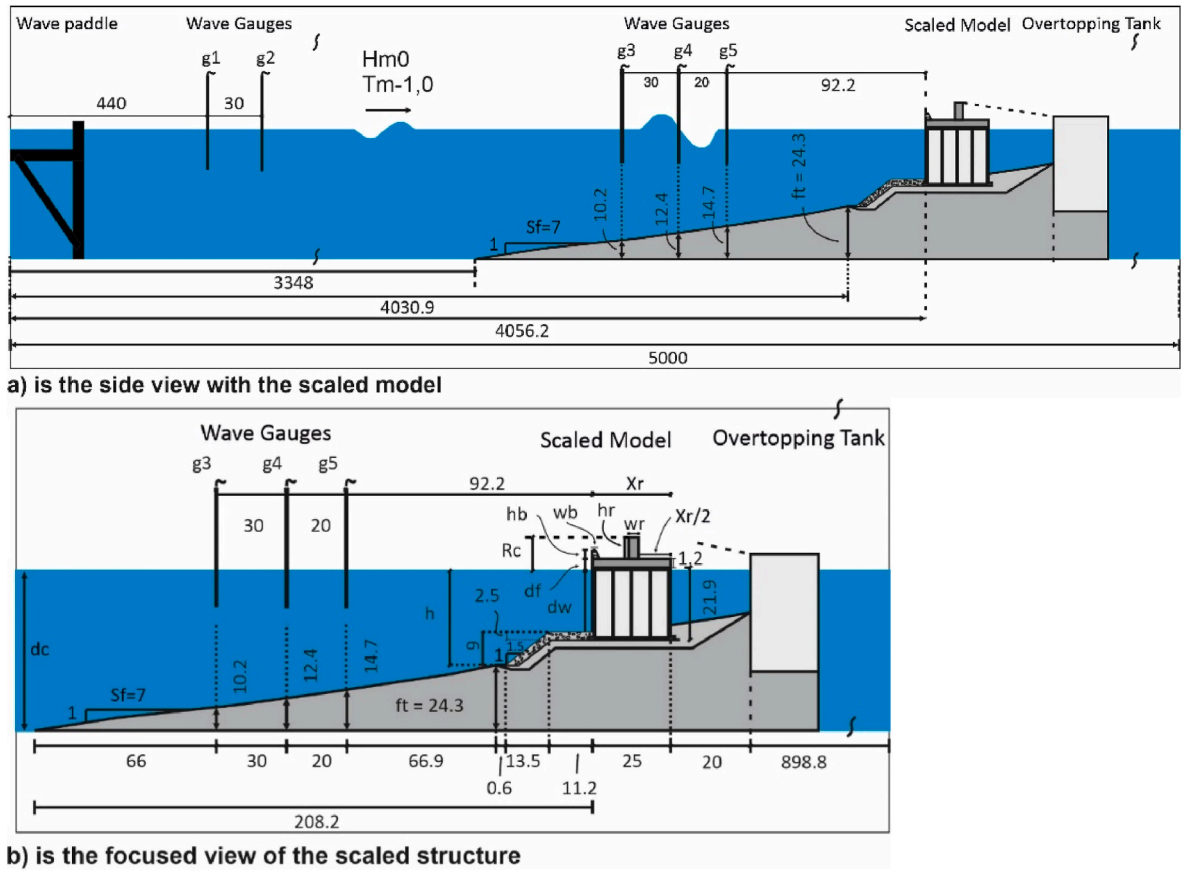

Fig. 5. Flume model set-up, used for irregular wave tests (composite vertical seawall, Italy). a) is the side view of the scaled model set-up, b) is the focused view of the scaled structure.

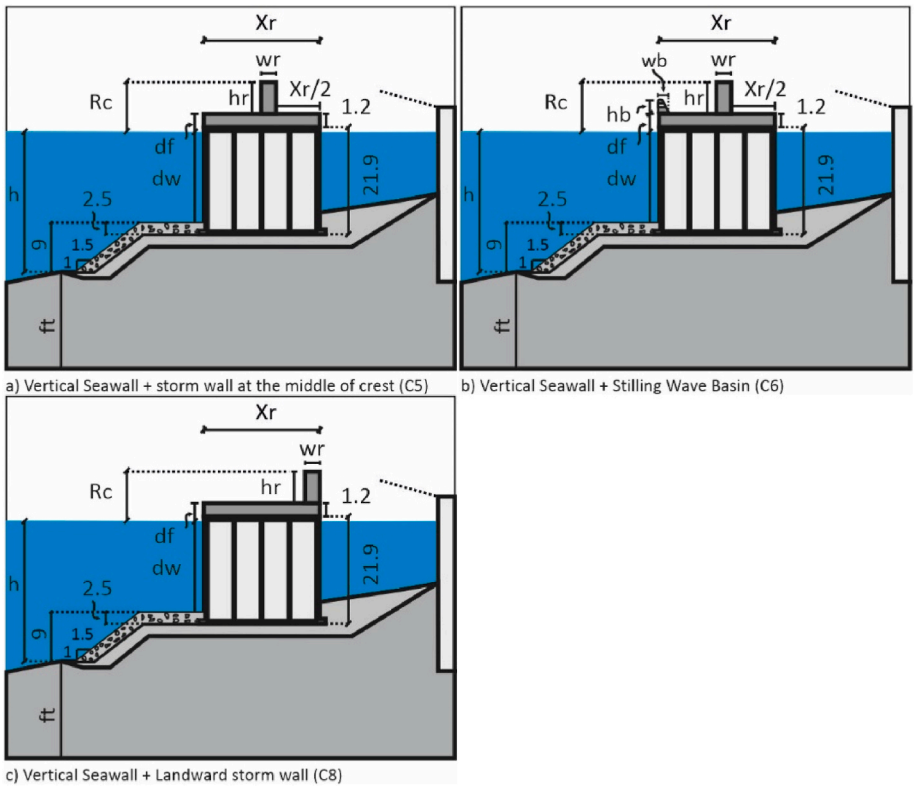

Fig. 6. Scaled models of the different superstructures tested in the study (composite vertical seawall, Italy).

Fig. 7. Details of composite vertical seawall in Italy.

$$\frac{q}{\sqrt{g.H_{m0}^3}} = 0.054.exp\left[-\left(2.12\frac{R_c}{H_{m0}}\right)^{1.3}\right] \quad (14)$$

For the rest of the test conditions, the steep foreshore transformed the waves significantly, therefore, the composite structure is limited to the rubble mound base and the seawall, and the steep slope in front of the mound is the foreshore of the structure. However, the mound in front of the vertical seawall is found to have no effect ($d \geq 0.6h$) for the test conditions. EurOtop (2018) states that the composite structure with influencing foreshore but without mound effect can be assumed as a simple vertical wall with an influencing foreshore. Therefore, the prediction formulas would be selected based on the impulsiveness of the wave conditions. For the impulsive test condition, I10, Eqs. 12, and 13 represent the reference case as well. The rest of the test conditions (I3, I7, I8, I9, I11, I22) are non-impulsive ($\frac{h^2}{H_{m0} \cdot L_{m-1,0}} > 0.23$), therefore, Equation (15) (increase the average discharge by about one standard deviation) should be used to determine the overtopping discharge as the reference value.

$$\frac{q}{\sqrt{g.H_{m0}^3}} = 0.062exp\left(-2.61\frac{R_c}{H_{m0}}\right) \quad (15)$$

As a result, the reference trendline for the experiments of the composite vertical wall is the best fit line based on the overtopping values calculated from three different formulae in EurOtop (2018). A single function is not provided for this composite reference line in this study as this reference trendline is based on the test conditions of the specific case study. Therefore, in the figures and discussions, this line will be denoted as Reference Trendline. Only the I10 test condition uses the same reference curve as the simple vertical wall (the first reference case) therefore discussion on the influence of the superstructures is only based on the calculated reduction factors (relative to their reference conditions).

The measured overtopping data of the test cross-sections of both experiments was plotted in a semi-logarithmic graph as dimensionless parameters; relative freeboard (R_c/H_{m0}) on the horizontal axis and relative overtopping discharge ($\log q/((gH_{m0}^2)^{0.5}(H_{m0}/d_w s_{m-1,0})^{0.5})$) on the vertical axis (Fig. 8). The results show that a promenade (case i) on a vertical seawall provides very little reduction. While single storm walls

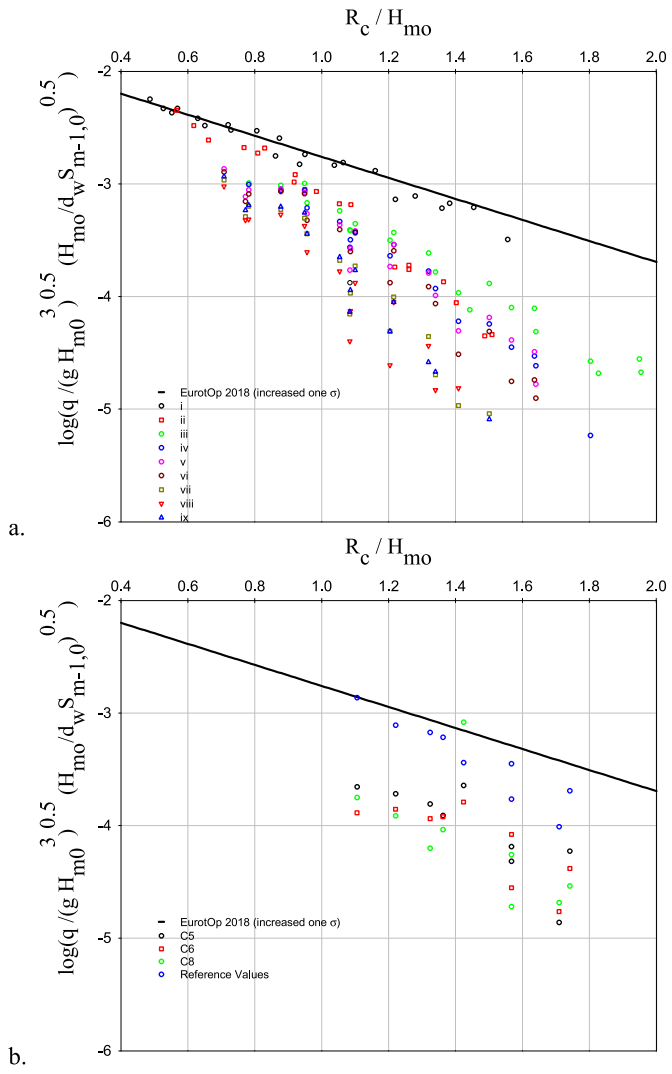

Fig. 8. Change in relative (dimensionless) overtopping discharge data due to superstructures with respect to relative freeboard with respective reference trendlines for a. simple vertical wall (reference line represented by EurOtop (2018) b. composite vertical wall (reference line based on the best fit of predicted values by EurOtop (2018)).

and parapet combinations reduce the overtopping at least 10 times, SWB configurations (cases v-viii, C6) reduce the overtopping significantly under the same hydrodynamic conditions used in the model tests. The effectiveness of superstructures increases significantly as the relative freeboard gets larger.

4.2. Reduction factors of the crest modifications

Reduction factors of the crest modifications are computed by comparing a fit through the measured overtopping data to the reference trendlines determined in Section 4.1. These reduction factors reflect how much each data point of the measured overtopping value would have to be shifted on the Y-axis to be exactly on the reference line. These reduction factors are to be included in the prediction formulas of EurOtop (2018) by modifying the relative freeboard $\left(\frac{R_c}{H_{m0}}\right)$ as $\left(\frac{R_c}{H_{m0}}\frac{1}{\gamma^*}\right)$ where γ^* is the reduction factor of the crest modification (selected superstructure) to provide an accurate prediction of the overtopping discharge for the vertical wall with the superstructure.

Fig. 9 and Fig. 10 show the collected overtopping data (on the left) and the calculated reduction factors (on the right) for each case under the test conditions. The datasets are assessed in two groups based on the high and low freeboard conditions; therefore, two ranges of reduction factors were evaluated when data is available. The trend line of each group (high and low freeboard conditions) is used to describe the reduction factor for a specific crest modification and the relative freeboard condition. Although the crest level depends on the geometry and water depth (i.e. there exist different crest heights); using dimensionless parameters ensures that the developed reduction factors are generally applicable as the trend of the dataset is accurate. However, a direct comparison of each data across different cases could not be possible.

The left panels in Figs. 9 and 10 also show the predicted overtopping values calculated by applying the reduction factors into the prediction formula of EurOtop (2018) (blue line). It is seen that the prediction formula with reduction factors (blue line) fits the measured data, but scatter increases for SWB configurations (cases v-viii, C6) as the physical process becomes much more complex. The observations also showed that green water type and splash type overtopping exists under the range of conditions tested for SWB cases that further increases the complexity of the dataset (Kisacik et al., 2019).

The right panels of Figs. 9 and 10 also present the trendlines based on individual reduction factors for every crest modification. These trendlines show that the reduction factors are influenced by changes in relative freeboard, particularly for high crested cases. For the simple vertical wall cases, the reduction factor decreases (less overtopping) as the relative freeboard increases. However, this influence is less significant for low crested conditions of the storm wall behind a promenade (cases iii and iv). On the other hand, for the composite vertical wall cases, reduction factors increase (reduction in overtopping is less) as relative freeboard increases. Based on the dataset of this study, the type of vertical wall (simple or composite) influences the overtopping behavior and the reduction factors of the same type of superstructures. This result could be significant in terms of design and adaptation measures of different types of vertical structures under impulsive and non-impulsive conditions however more detailed research and the dataset are needed to be able to present general conclusions.

The reduction factors of each superstructure tested in this study are defined by equations (Eq. (16)) based on the relative freeboard condition using the trendlines presented in Figs. 9 and 10.

$$\gamma = k + l\frac{R_c}{H_{m0}} \tag{16}$$

Coefficients of k and l are determined based on the relative freeboard condition (low crested or high crested) based on the classification of the test data of each superstructure (Table 4). For cases, vii and viii, very limited data exist for the high-crested condition therefore, no formula is proposed. For composite vertical wall cases (Table 5), the whole dataset is used to determine one equation to represent reduction factors due to the limitation of the dataset.

The reduction factors show that the seaward storm wall under lower freeboard conditions is not as effective as a landward storm wall at the end of a promenade (case ii and iv). However, under higher freeboard conditions, both cases provide a similar reduction in the overtopping behind the superstructure. The effect of parapet becomes important as the performance of case ii is better than case iii (no parapet) but very similar to case iv (with parapet) (see also Fig. 9). The range of the reduction factors shows that there is a certain amount of scattering for the proposed Eq. (16). Cases iii, iv, v, and vi show similar effectiveness for low crested conditions whereas there is a distinct change in effectiveness for higher relative freeboard. These results also indicate that changes in the seaward configuration for crest modifications significantly influence the overtopping discharge under higher relative freeboard conditions. For low crested conditions, SWB configuration (case v, vi) and promenade and storm wall combination (case iii, iv) provide a similar reduction in overtopping. However, the conditions over the promenade are significantly different among these four cases as SWB blocks much of the energy of the wave impact but not the amount of

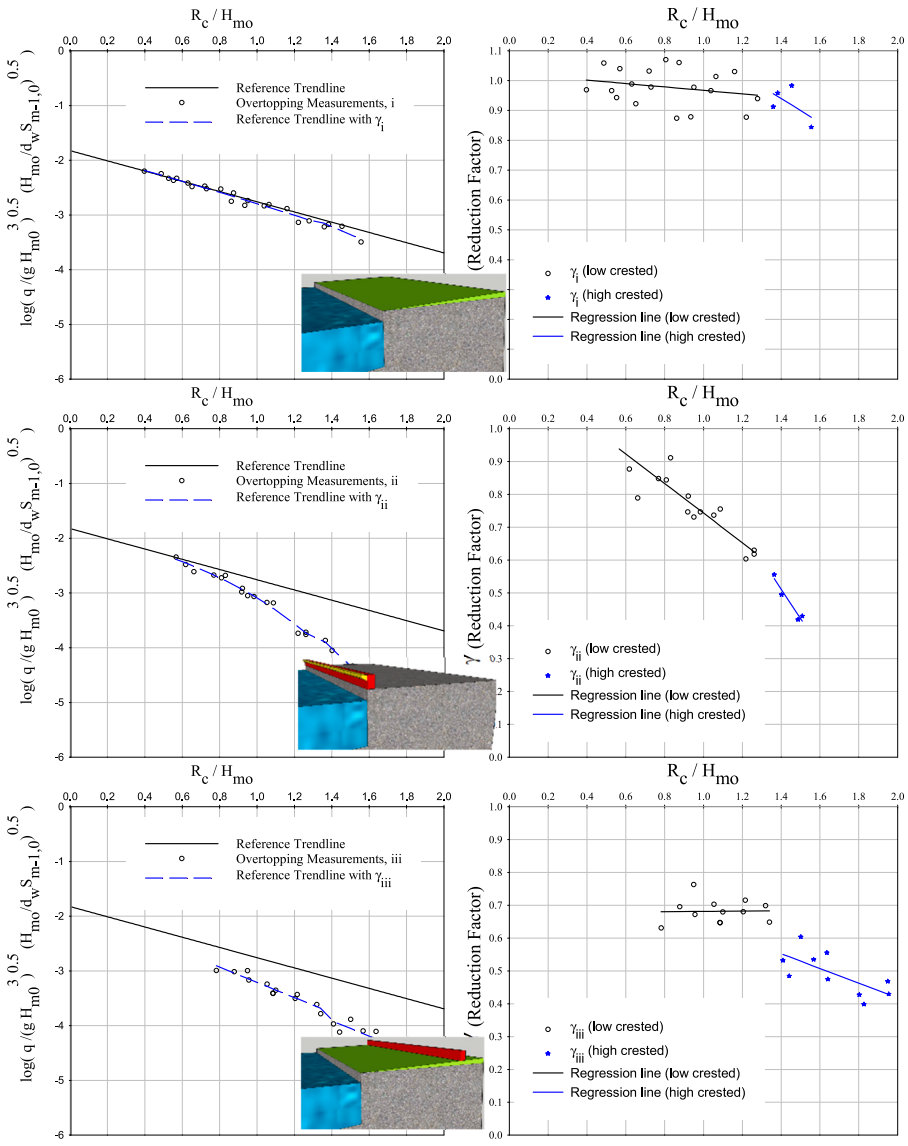

Fig. 9. Overtopping discharge results for each test (left panel) and the reduction factors calculated with trend lines (right panel) for cases based on a simple vertical wall.

overtopping.

For the composite vertical structure, the reduction factors show that a storm wall end of a promenade (C5) provides less reduction than the crest modifications based on stilling wave basin with one row of seaside storm wall (C6). It is observed that for a single row stilling wave basin superstructure (C6), the blocking coefficient (C_b) is too high in this experiment, which reduces the effectiveness of the design due to less back drainage from the promenade between waves. On the other hand, the landward storm wall at the end of the longer promenade (C8) reduces the overtopping further. Comparison of C5 and C8 show the significant effect of basin width as C8 is more effective in reducing the overtopping when storm wall height is kept constant.

Comparison of these superstructures for composite vertical walls and simple vertical walls indicates that similar superstructures provide different levels of reduction in overtopping. Although direct comparison is not possible among the cases due to different geometries, the reduction factors for superstructures of the composite vertical wall are much higher than the factors of similar superstructures on a simple vertical wall (case ix vs C6, case iii vs C5 and C8) under same freeboard conditions. This could be another indication that the type of vertical structure and the wave-structure interaction (the impulsive/non-impulsive conditions) have a significant influence on the performance of different superstructures.

These formulas of reduction factors for a particular case only represent the effect of relative freeboard on the configuration of the crest modifications. They do not reflect directly the possible changes in the geometry of the parameters such as promenade width, wall height, or parapet angle as these parameters were kept constant throughout the tests.

5. Discussions

5.1. Influence of promenade

Case i provides a reduction factor for a selected promenade geometry (2% slope and 8 m of prototype width) based on a relative freeboard (Table 4, Fig. 9). However, the reduction factor for a promenade on dikes in EurOtop (2018) depends on the width of the promenade. Although the width of the promenade is kept constant for the tests in this study, the range of hydrodynamic conditions (6 different wave periods)

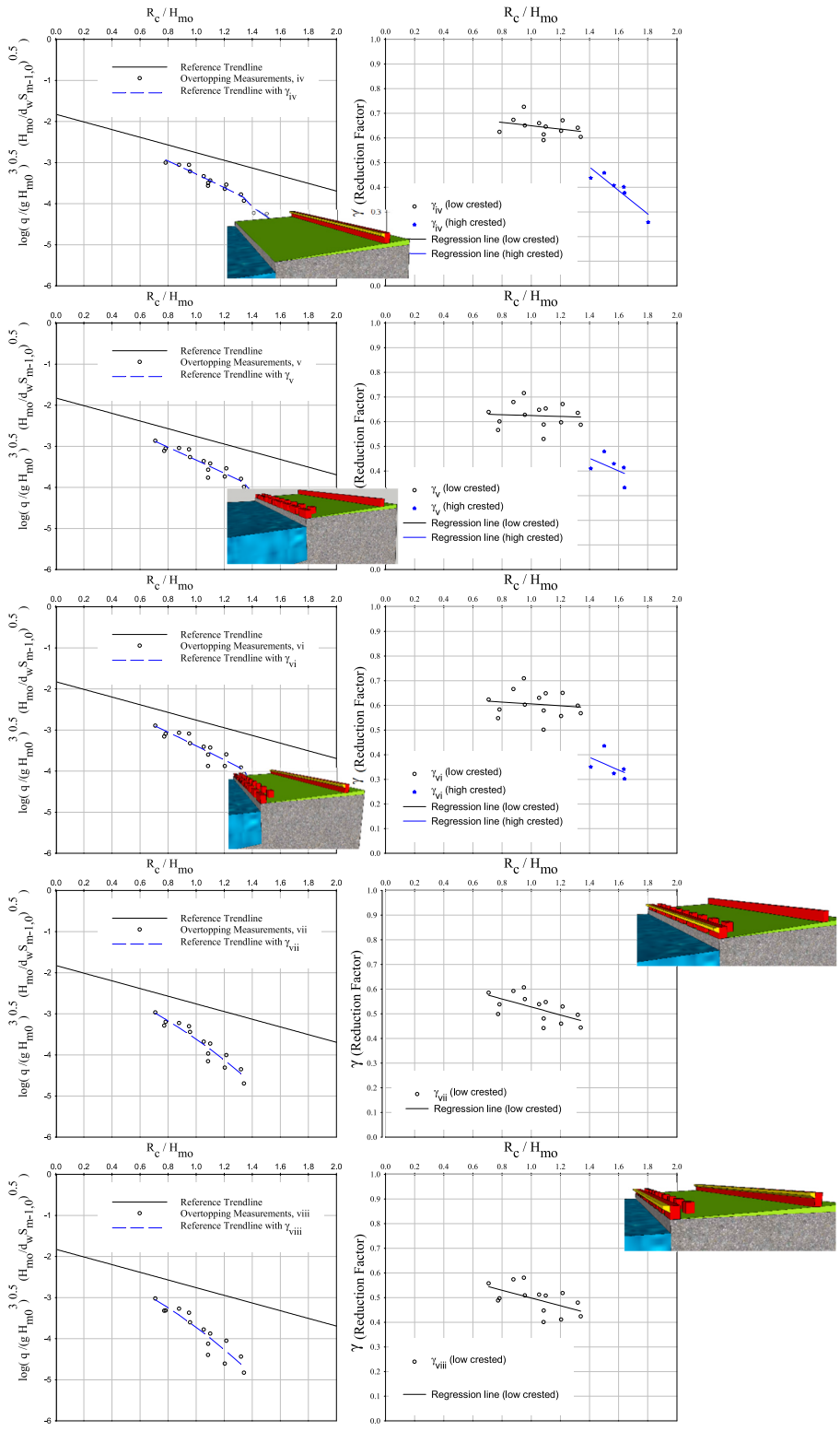

Fig. 9. (*continued*).

enabled an assessment of the influence of promenade width as a dimensionless parameter, $\frac{X_r}{L_{m-1.0}}$. Therefore, the reduction factor calculated for the reference formula is further analyzed following the formula proposed for dikes as shown in Fig. 11. The results show that there is a trend of reduction in overtopping as dimensionless promenade width increases. This indicates that wider promenades may reduce overtopping under the same hydrodynamic conditions. However, the scatter in the data also shows that promenade can contribute to higher discharge values ($\gamma_{promenade} > 1$). This could be a result of interaction between consecutive wave overtopping as the next overtopped wave moves along a promenade much easily due to the water layer from the previous discharge.

Although the trend line of results of experiments is very similar to the formula presented in EurOtop (2018) for dikes (Eq. (1) in Section 2), a

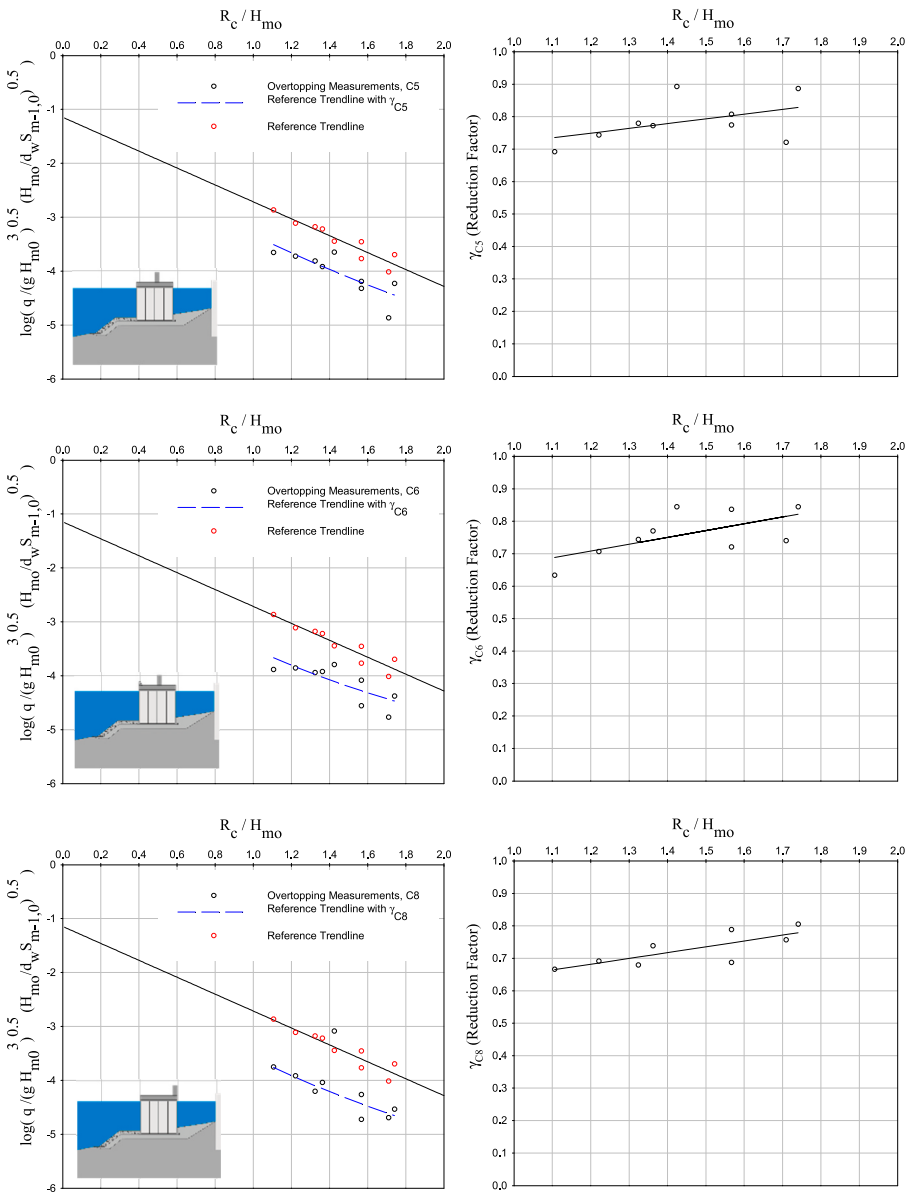

Fig. 10. Overtopping discharge results for each test (left panel) and the reduction factors calculated with trend lines (right panel) for cases based on a composite vertical wall.

Table 4
Coefficients of Equation (16) and the corresponding reduction factors for superstructures on the simple vertical wall.

Type	low crested (R_c/H_{m0} <1.35)			high crested (R_c/H_{m0} >1.35)		
	k	l	γ	k	l	γ
i	1.0252	−0.058	0.87–1.07	1.5039	−0.4028	0.84–0.98
ii	1.1932	−0.4502	0.60–1.01	1.7648	−0.8954	0.42–0.56
iii	0.6757	−0.0053	0.63–0.76	0.8664	−0.2245	0.40–0.60
iv	0.7166	−0.0674	0.59–0.73	1.1491	−0.4767	0.46–0.60
v	0.6414	−0.017	0.53–0.72	0.8113	−0.2571	0.33–0.48
vi	0.6439	−0.0383	0.50–0.71	0.7501	−0.2577	0.30–0.44
vii	0.6895	−0.1618	0.44–0.61	–	–	0.25
viii	0.655	−0.1569	0.40–0.58	–	–	0.28
ix	0.7454	−0.2139	0.45–0.63	–	–	0.24

similar equation for the reduction factor of the promenade on vertical structures is determined based on the dataset of case i of low crest freeboard conditions:

Table 5
Coefficients of Equation (16) and the corresponding reduction factors for superstructures on the composite vertical seawall.

Type	k	l	γ
C5	0.1466	0.573	0.89–0.69
C6	0.2099	0.4562	0.84–0.63
C8	0.1796	0.4661	0.81–0.67

$$\gamma_{promenade\_low-crested} = 1 - 0.29\frac{X_r}{L_{m-1,0}} \; for \; 0.08 \leq \frac{X_r}{L_{m-1,0}} \leq 0.21 \tag{17}$$

However, the scatter of the dataset shows the necessity for a larger data set and experiments with different promenade widths.

5.2. Influence of landward storm wall at the end of the promenade

The combination of promenade and landward storm wall is discussed for dike crest modifications as the geometry can be frequently observed

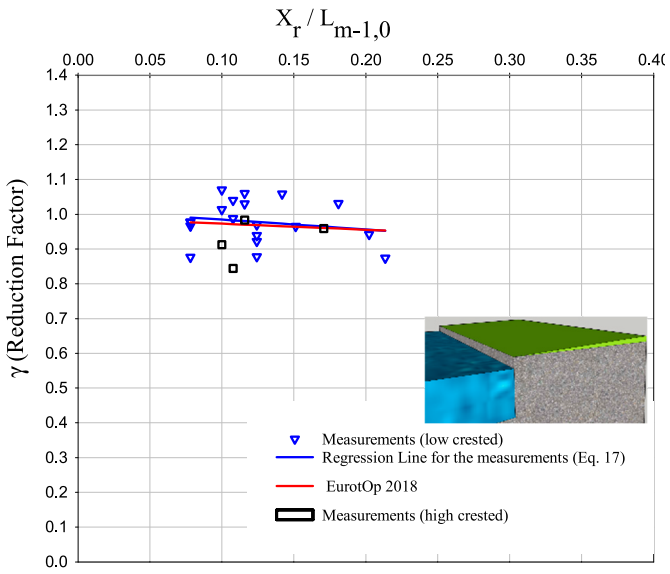

Fig. 11. Vertical seawall with promenade – reduction factors for dimensionless promenade width.

around the world. Three cases in this study present this combination for vertical structures. Case iii of the simple vertical wall experiments and C5 and C8 of composite vertical wall experiments are similar in their layout but with different storm wall heights and promenade widths. C5 configuration has half of the promenade width of C8 with the same wall height. The datasets and the reference trend lines for each experiment group are presented in Fig. 12. Both of the reference trendlines are shown in this figure to highlight the level of reduction respectively.

It is shown in the previous section that the simple promenade has little influence on the reduction of overtopping especially if the width is limited. The inclusion of the landward storm wall significantly influences the overtopping discharge. This superstructure (independent of dimensions) is more effective compared to a seaward storm wall (with or without parapet) and a promenade combination for lower relative freeboard values. On the other hand, the trend lines of C5 and C8 indicate that a wider promenade (C8) reduces the overtopping more. However, the scatter of the data also shows that the significance is

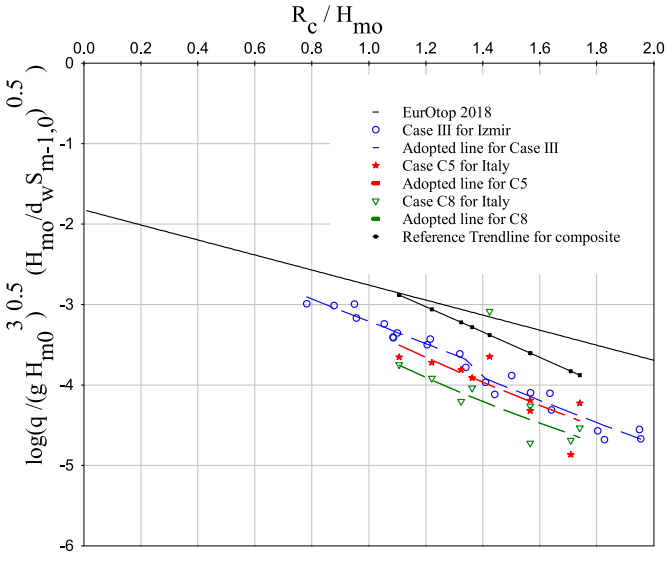

Fig. 12. The relative overtopping discharge (logarithmic scale) plotted against the relative freeboard for cases that is a combination of a promenade and a landward storm wall.

limited when case iii datasets within the same range of relative freeboard values of C5 and C8 are compared. Although the range of dimensionless promenade width ($X_r/L_{m-1,0}$) of Case iii is similar to C8 for the same range of relative freeboard values, the overtopping values are lower for C8. This difference could very well be due to the difference in storm wall heights as Case iii has much lower relative wall height values ($h_r/R_c < 0.38$) than C8 ($h_r/R_c = 0.80$). Although the height of the storm wall is included in relative freeboard inherently (definition of freeboard includes the wall height), this result could indicate that the influence of storm wall height might be prominent in the performance of the combined geometry as this elevation change occurs a distance away from the vertical wall of the main structure. This argument also indicates that while it is important to understand the influence of the components of a superstructure to determine the dominant processes, it would not be accurate to assume that these processes are independent. It can also be argued that the order of overtopping reduction due to a landward storm wall at the end of a promenade as a combination could be described mostly with hydrodynamic conditions (impulsive/non-impulsive) rather than the dimensions of the parts of the combinations such as promenade width or height of the storm wall.

5.3. *Influence of parapets*

The influence of parapet on overtopping for vertical seawall is one of the crest modifications discussed in EurOtop (2018). Reference case (SSW of Kisacik et al., 2019) and SSW with Parapet (ii) cases are used to compare the effect of the parapet on the seaside storm walls (Fig. 13). For both cases (SSW and SSW with parapet), the same horizontal promenade exists before the overtopping tank, therefore the overtopping values also include the effect of this horizontal width. As the only geometrical difference between the two cases is the parapet on the seaward storm wall, the difference in overtopping values is expected to be due to the parapet. Then, LSW case (iii) and LSW with Parapet (iv) are compared to show the parapet effect on the landside storm wall whereas case iii is the reference case for the comparison. Similar to seaward parapet comparison, the landward storm wall is located at the end of the promenade (%2 slopes of constant width) for both cases, iii and iv, and the overtopping tank is located behind the landward storm wall (Fig. 13). Therefore, the overtopping values collected for both cases iii and iv also include the effect of promenade however the only geometrical difference between the cases is the parapet which is expected to be reflected in the differences of overtopping values of case iii and case iv. The reduction in the overtopping data for both comparisons is used to assess the performance of the approaches proposed by EurOtop (2018) for parapets on vertical seawalls (see Fig. 14).

Fig. 14 shows that reduction in overtopping due to parapet is also influenced by relative freeboard conditions. Here, the reduction factors are computed by comparing the measured overtopping date of SSW and LSW with Parapets to the data of SSW and LSW without parapets discussed in Fig. 13. Different than the reduction factors computed in section 4.3, these reduction factors reflect only parapet effects. Fig. 14 shows that higher relative freeboards reduce overtopping effectively than lower freeboard conditions. It is also seen that the seaside storm wall with parapet has a much larger influence on the wave overtopping than a landside storm wall with a parapet at the end of a promenade. The parapet on the seaside storm wall diverts the upward jet of wave impact thus reducing the overtopping. On the other hand, the overtopping volume approaches the landward storm wall like a surging wave and there is no upward jet motion for the parapet to divert. Therefore, the effect of the parapet on the landward storm wall is limited.

In Fig. 14, the red line indicates the reduction factor values calculated using of EurOtop (2018) equation for parapet (Eq. (8) in Section 2). However, this set of reduction factors proposed by EurOtop (2018) does not represent our results well. The range of reduction factors for relative freeboard between 0.5 and 1 can be used to represent the parapet effect on the seaside storm wall for the same freeboard range. But the proposed

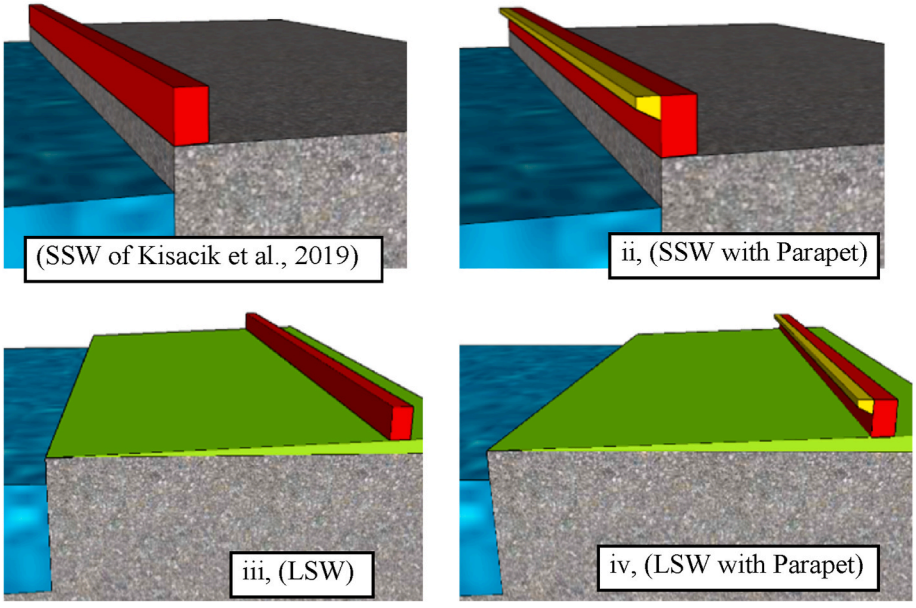

Fig. 13. Crest modifications used in the assessment (top panel on seaward storm wall and bottom panel on landward storm wall).

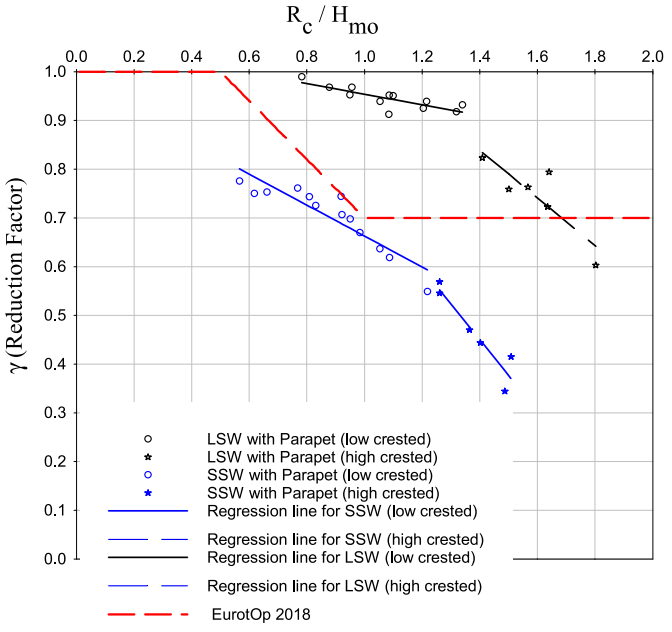

Fig. 14. Variation of the reduction factor plotted against the relative freeboard for different configurations of parapet - the reduction factor of EurOtop (2018) in red. LSW – Landward Storm Wall; SSW – Seaward Storm Wall. (For interpretation of the references to colour in this figure legend, the reader is referred to the Web version of this article.)

factors can not be used to represent parapets on landside storm walls. EurOtop (2018) does not differentiate the reduction factor of parapet for a storm wall based on its location but only considers the change in crest height due to parapet. However, it is observed that the location of the parapet determines the efficiency of the parapet as the type of overtopping changes for different locations along the promenade and landside storm wall combination as discussed previously. Therefore, another set of reduction factor formulas (Eqs. (18)–(21)) for parapet on seaside storm wall (SSW) and landside storm wall (LSW) are proposed based on the dataset generated by physical experiments. Similar to previous reduction factor assessments, the formulas are based on low crested and high crested freeboard configurations.

SSW and Low Crested

$$\gamma_{prapet\_SSW\_low-crested} = 1 - 0.32\frac{R_c}{H_{m0}}\ for\ 0.57 \le \frac{R_c}{H_{m0}} \le 1.22 \quad (18)$$

SSW and High Crested

$$\gamma_{prapet\_SSW\_high-crested} = 1.5 - 0.73\frac{R_c}{H_{m0}} for 1.26 \le \frac{R_c}{H_{m0}} \le 1.52 \quad (19)$$

LSW and Low Crested

$$\gamma_{prapet\_LSW\_low-crested} = 1.1 - 0.11\frac{R_c}{H_{m0}}\ for\ 0.78 \le \frac{R_c}{H_{m0}} \le 1.34 \quad (20)$$

LSW and High Crested

$$\gamma_{prapet\_LSW\_high-crested} = 1.5 - 0.49\frac{R_c}{H_{m0}}\ for\ 1.41 \le \frac{R_c}{H_{m0}} \le 1.80 \quad (21)$$

These formulas are based on relative freeboard and the location of the storm wall, however, they do not consider the geometry of the parapet such as the parapet angle. For all the cases (case ii and iv), parapet geometry is kept constant. However, for a comprehensive set of formulas, the possible influence of parapet angle, width, and other parameters need to be considered.

Additionally, experiment results were compared to the calculated k_{bn} (Eq. (9) in Section 2) based on EurOtop (2018). Fig. 15 shows that this approach represents the model results fairly well for the whole range of experiments. However, the predicted overtopping values would be higher than the experiments, which makes this approach a conservative one. The representability of this approach is limited for very low k_{bn} values and this is also reflected in Fig. 15.

5.4. Influence of SWB components

Stilling Wave Basin configuration has a lot of components such as the number of rows of storm walls, the height of storm walls, the blocking coefficient of seaward storm walls, and the width of the basin. Parapets on storm walls can also be included in the design. All these factors are included in the reduction factor of SWB configurations, and interdependency is very prominent. Kisacik et al. (2019) presented an optimization study to demonstrate the effect of individual parameters for the

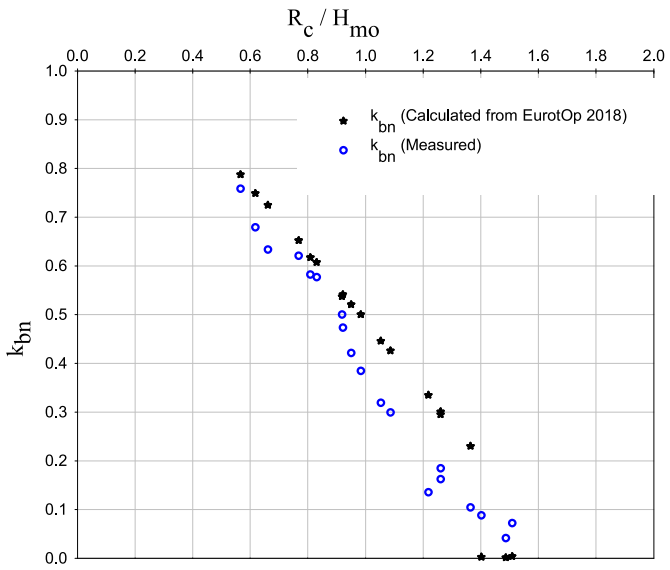

Fig. 15. Variation of the reduction factor (k_{bn}) plotted against the relative freeboard for different configurations of the parapet and the reduction factor calculated using EurOtop (2018) (Eq. (10)).

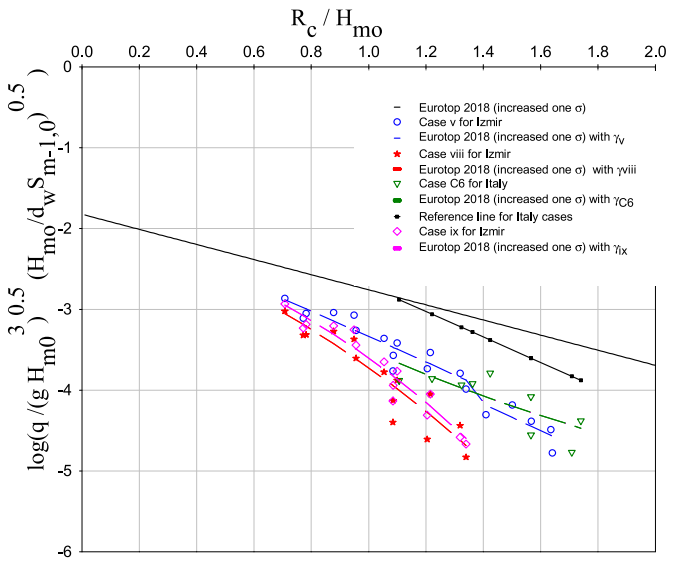

Fig. 16. The relative overtopping discharge plotted against the relative freeboard for selected SWB cases with the two reference trendlines for the simple vertical wall (EurOtop, 2018) and composite vertical wall conditions (Reference Trendline).

reference case of Izmir. The results of the optimization study showed that there is an optimum blocking coefficient as low blockage means larger volumes of water in the basin reaching the landward storm wall and high blockage means slower drainage of the basin which causes larger volumes of water in the basin. Similarly, the effect of the width of the basin also converges to an optimum value such that basins wider than this optimum width do not contribute to the reduction significantly. But it is shown that narrow basins have a disadvantage over wider basins when all the other components are kept constant. The height of the storm walls affects the crest freeboard therefore this parameter is significant for SWBs as well as for most of the crest modifications.

In this study, six different SWB configurations are presented. Four of these SWB cases are compared to provide a discussion on the importance of the interdependency of components of SWB, albeit with limited data. Still, this comparison would highlight the fact that composite reduction factors could only be valid for certain SWB geometries and it is difficult to provide universal reduction factors for SWBs compared to other crest modifications. C6 of composite vertical wall experiments is a single row SWB with a narrow basin whereas case ix of the simple vertical wall is a single row SWB with a wider basin. Case v is a double row SWB with the same basin width as case ix. Case viii has the same layout as case v but with parapets on seaward and landward storm walls. Although the cases presented in Fig. 16 have many differences in their configurations, the combined reduction effect of these differences can be discussed.

Fig. 16 shows that under similar hydrodynamic conditions (R_c/H_{m0}), overtopping values of C6 and case v are similar to each other even if case v has a double row setup and a wider promenade which would provide higher reductions in overtopping. But the higher landward storm wall height of C6 might be the reason for similar values as the combination of the components determines the overall reduction. Although case ix and C6 are both single row cases, a direct comparison is not possible as case ix has a parapet that strongly influences the overtopping behavior as discussed in Section 5.3. Still, a higher landward storm wall of C6 compared to case ix would be expected to reduce the overtopping as a landward storm wall is a last and final component to determine the total overtopping for SWBs. However, C6 has a lower seaside storm wall, narrow basin width, a very large blocking coefficient, and no parapet compared to case xi. Therefore, the combination of case ix provides a larger reduction in the overtopping compared to C6. These results further demonstrate that the composite reduction factors should consider the interdependency of components of complex geometries and the performance of SWB depends on this interdependency significantly.

5.4.1. *Comparison of single and double row shifted storm walls on the seaside*

The influence of single and double-row storm walls on the seaside can be highlighted by comparing the overtopping measurements taken under the case viii and case ix. Both the first row and single row of seaside storm walls have parapets and the landside storm wall. The crest height of both cases is the same as the promenade of the same width acting as the basin as shown in Fig. 17.

The results of both cases presented in Fig. 18 are compared to the reference equation. There is only one data for high freeboard conditions whereas the rest of the data is used to determine the coefficients of the reduction factor equation (Table 4). These results show that single row SWB configuration (case ix) performs slightly less effectively than double row SWB (case viii). Therefore, case ix could also be an effective measure to reduce the overtopping on vertical seawalls. However, implementing a single row SWB could introduce risks to humans and vehicles along the promenade as the jets through the single rows could directly hit the users whereas double shifted rows diminish this process significantly.

5.4.2. *The parapet effect on SWB configurations*

Fig. 19 shows the trend lines of measured data of cases v to viii which are all SWB configurations with a reference line for the simple vertical wall (EurOtop, 2018). The red line is the predicted overtopping values using the reduction factor proposed by Kisacik et al. (2019) for a specific SWB configuration of double shifted seaward storm walls and a recurved storm wall at the end of a promenade on a simple vertical wall (Eqs. (10) and (11) in Section 2). Although this configuration presented by the red line is not tested as part of this study, the crest height and the basin dimensions are the same as the cases compared in this study. The difference between these SWB cases is the placement of parapets on the storm walls.

The results show that the placement of the parapet on the seaside storm wall (cases vii and viii) reduces the overtopping the most compared to all other locations. Parapet only on the landside storm wall (case vi) decreases the overtopping slightly regardless of the presence of a parapet on the seaward storm wall. Both storm walls having parapet

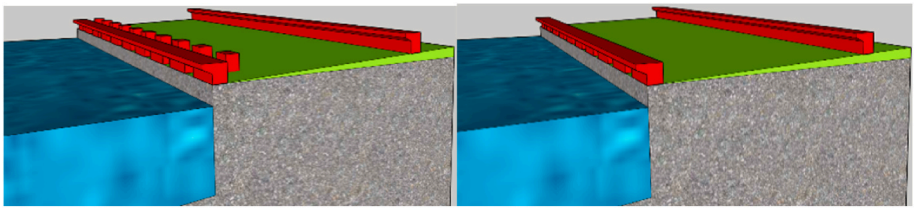

Fig. 17. Configuration of double row SWB (left) and single row SWB (right).

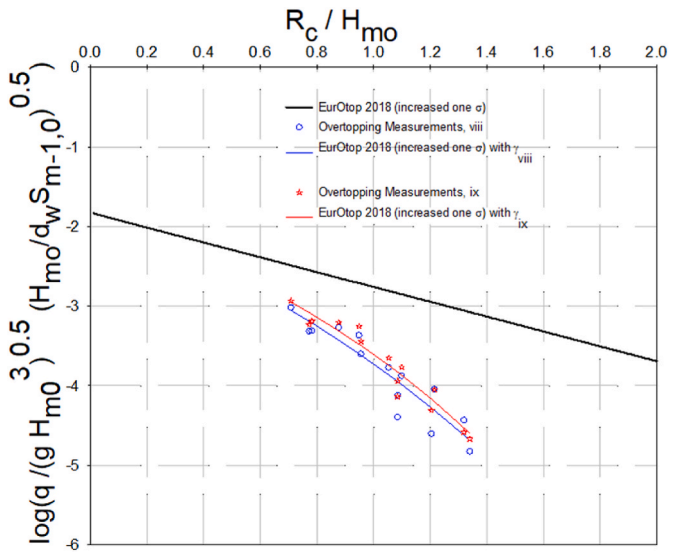

Fig. 18. Variation of the relative (non-dimensional) overtopping discharge plotted against the relative freeboard for single and double row SWB.

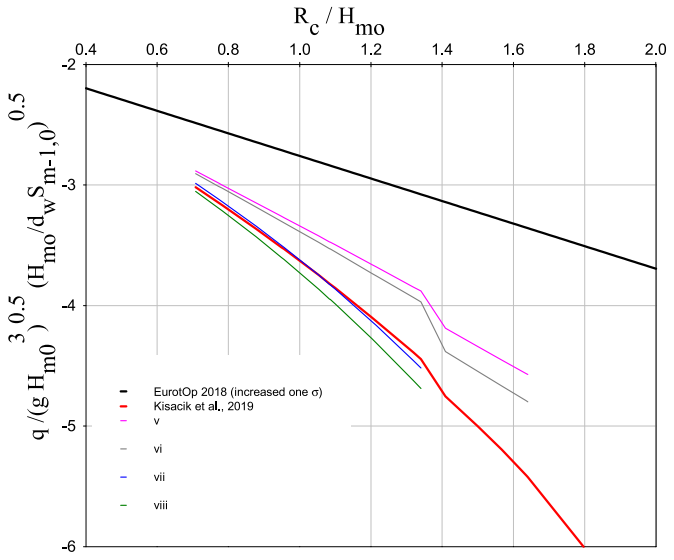

Fig. 19. Variation of the relative (non-dimensional) overtopping discharge (logarithmic scale) plotted against the relative freeboard for different SWB configurations including the SWB setup tested in Kisacik et al. (2019) (red line). (For interpretation of the references to colour in this figure legend, the reader is referred to the Web version of this article.)

(case viii) cause the least overtopping, however, the difference to case vii (the parapet on seaside storm wall only) is small.

The setup of Kisacik et al. (2019) (red line) is similar to case vi of this study which has a parapet on the landward storm wall only. However, the overtopping values predicted by the reduction factor proposed by Kisacik et al. (2019) are significantly lower than those of case vi but much closer to case vii where the overtopping is affected by a parapet on seaside storm wall. This difference could be because of the recurved shape of the landward wall in the SWB setup of Kisacik et al. (2019) where the complete landward storm wall acts like a parapet. This shape could reduce the overtopping significantly more than a small parapet on a storm wall. Therefore, the overtopping values are closer to the case with a parapet on the seaward storm wall where significant reduction is observed.

5.5. Relationship between the reduction factors of the different superstructure components

The cases tested during physical experiments also provided a set of data to assess the possibility of calculating composite reduction factors from individual reduction factors of superstructure elements such as a parapet. Tuan (2013) mentions that in the literature, the total effect on wave overtopping reduction can be calculated as the product of all contributing components. Therefore, it is possible to derive composite reduction factors if individual factors are known. On the other hand, Van Doorslaer et al. (2015) opposes this approach and show that simple multiplication of individual factors would not estimate the actual reduction in wave overtopping. Both discussions consider a combination of different elements such as a composite reduction factor that combines promenade and storm wall.

In this paper, for this discussion, the selected reference configuration is SWB without parapet and the composite reduction factor includes the cases as shown in Fig. 20:

1) SWB plus two parapets, respectively on seaside and landside storm wall (γ_3).
2) SWB plus parapet on the landside storm wall (γ_1).
3) SWB plus parapet on the seaside storm wall (γ_2).

Therefore, the question is if multiplication of reduction factors of first and second cases would provide a similar reduction factor for the final case (γ_3) (Eq. (22)).

$$\gamma_3 = \gamma_1 * \gamma_2 \tag{22}$$

Fig. 21 shows the results based on the experimental data. The multiplication of the two individual factors provides an accurate representation of the composite factor for low crested conditions in the agreement with the discussion of Tuan (2013). A similar discussion is not possible for the high crested condition due to limited data.

However, in this case, the composite reduction factor is calculated to determine the total parapet effect using individual parapet effects, not different elements with different mechanisms to change the overtopping discharge. Therefore, the recommendation of Van Doorslaer et al. (2015) could be still valid, especially for situations where the physics change between a wave overtopping a structure and an overtopping bore on the promenade overtopping a storm wall.

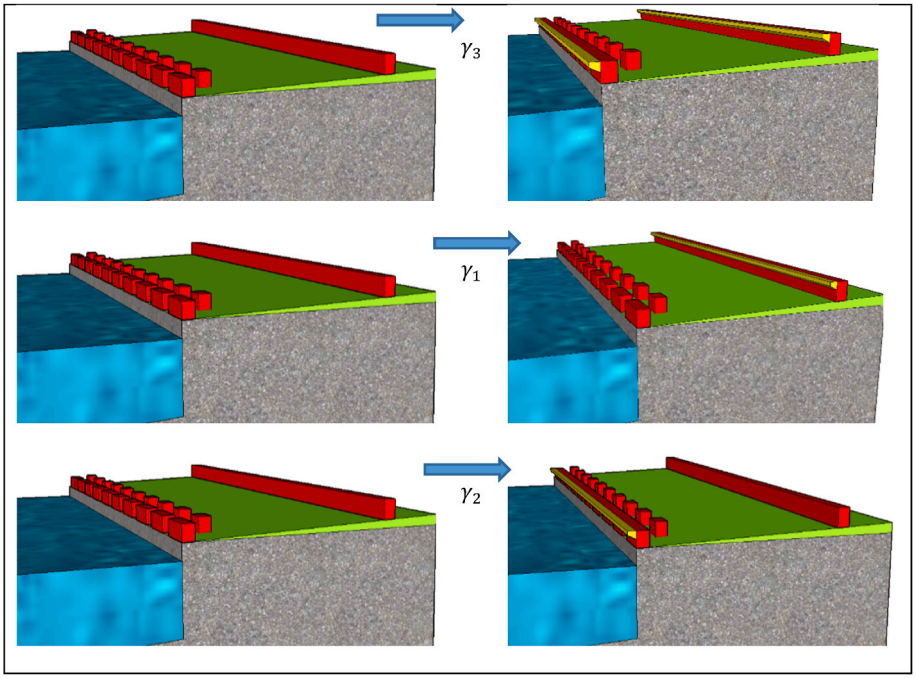

Fig. 20. Configurations used in the assessment of reduction factors of combined structures.

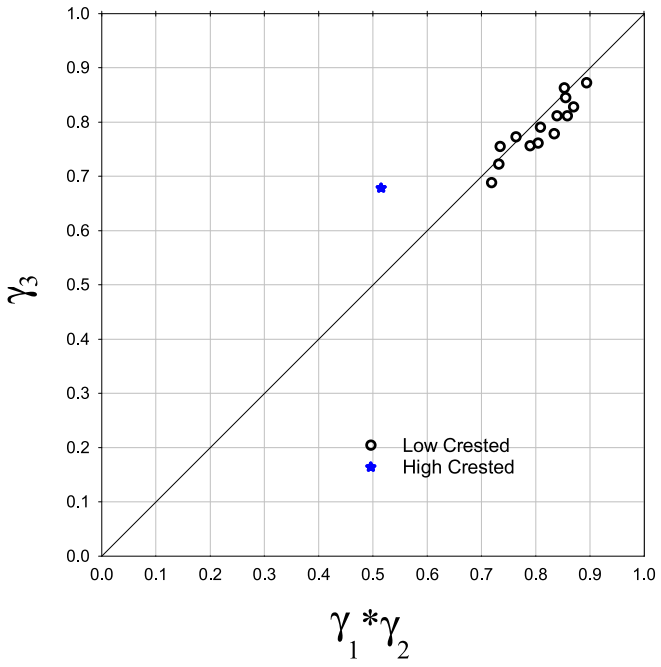

Fig. 21. Composite reduction factor and the product of individual factors.

6. Conclusions

To investigate the reduction of overtopping by crest modification of vertical seawalls, two independent physical model studies are presented that cover a variety of hydrodynamic conditions. These experiments enhance the limited dataset regarding crest modifications for vertical structures, both simple and composite vertical structures. Data from the first model study covers impulsive conditions over a simple vertical seawall with influencing foreshore while the second model study is a composite vertical structure with a very steep foreshore. The second study mostly has non-impulsive conditions due to the steep foreshore. The crest modifications tested include a promenade, storm wall behind a promenade, parapets, and different stilling wave basin geometries such as single row/double row seaside storm wall configuration. The crest modifications are selected to represent conditions where modifications are needed for an existing vertical structure under higher extreme water levels due to climate change. As increasing the crest heights of existing structures might not be possible due to the present use of these structures, the performance of these selected superstructures could provide alternative solutions.

Several reduction factors have been proposed in this paper, however, each of them is applicable for the model geometry and within the test conditions. These reduction factors could be included in the formulas presented in EurOtop (2018) to calculate the average overtopping discharge for the respective geometry, wave, and relative freeboard conditions. Even though the use of these factors is limited to the test characteristics, comparing the performance of different crest modifications especially for lower relative freeboard conditions is important for adapting the future sea levels. With increases in sea level, the existing relative freeboard conditions will become lower, and the overtopping increases accordingly for the simple vertical wall tests which show impulsive overtopping conditions. Therefore, most of the data presented in this study cover mostly lower ranges of relative freeboard for each of the geometries. On the other hand, the composite vertical wall results, which were mostly non-impulsive conditions, showed an opposite trend (reduction increased as relative freeboard decreased) which showed that the influence of superstructures is highly related to the wave-structure interaction (i.e., impulsiveness and the type of the vertical structure (simple, composite)). Therefore, crest modification of vertical structures is very complex, and impulsive and non-impulsive conditions should be assessed for the same superstructures to derive unified conclusions.

Among all the crest modifications tested in both studies, it is seen that a promenade on a vertical seawall provides very little reduction, whereas SWB configurations reduce the overtopping significantly. The results show that the seaward storm wall under lower freeboard conditions is not as effective as a landward storm wall at the end of a promenade. However, the effectiveness of the parapet and seaside storm wall increases significantly as the relative freeboard gets larger. A comparison of similar configurations with and without parapet shows

that the parapet helps to reduce the overtopping discharge and the increase in relative freeboard influences the effect of the parapet. However, the reduction introduced by a parapet on a single storm wall is not as effective as a change of the configuration of the superstructure from a storm wall to SWB. Moreover, the configuration of SWB is important as both double row seaside storm wall and larger basin width increase the reduction. However, the performance of different SWB configurations becomes similar (lower reduction of overtopping) as the relative freeboard decreases which is the expected change due to climate change as extreme water levels are expected to be increased. But compared to other crest modifications, SWB configurations perform better, especially compared to having only a seaside storm wall (even with a parapet).

Several formulae and approaches presented in EurOtop (2018) are used in the study that enabled the assessment of the applicability of the prediction formulas for different cases. The recommendation on including the steep foreshore as part of the structure and using the corresponding prediction equations for the enhanced geometry is tested in the second model study. The recommendation (if applied directly) assumes that the cross-section behaves like a simple vertical wall with no influencing foreshore. However, when the classification of overtopping formulas for composite vertical structures are applied to the test conditions, the majority of the tests were grouped as a composite vertical wall with influencing foreshore. This result was also reflected in the wave gauge analysis. Although the foreshore is very steep, most of the hydrodynamic conditions were highly influenced by the steep foreshore. Two different approaches proposed in EurOtop (2018) to determine the bullnose/parapet effect is tested with the model data. The k_{bn} parameter defined by EurOtop (2018) represents the model results fairly well for the whole range of experiments, although the predicted overtopping values would be higher than the experiments, which makes this approach a conservative one.

The cases tested during physical experiments also provided a set of data to assess the possibility of calculating composite reduction factors from individual reduction factors of superstructure elements such as a parapet. In the literature, two different arguments are presented whether the total effect on wave overtopping reduction can be calculated as the product of all contributing components or not. In this paper, the composite reduction factor includes two parapets on seaside and landside storm walls where the reference configuration is SWB without parapet and the final crest modification integrates parapets on both seaside and landside storm walls. The results based on the experimental data showed that the multiplication of the two individual factors provides an accurate representation of the composite factor for low crested conditions. However, in this case, the composite reduction factor is calculated to determine the total parapet effect using individual parapet effects, not different elements with different mechanisms to change the overtopping discharge. Therefore, the total effect on reduction not being equal to the product of all contributing factors is still valid especially for situations where the physics change between a wave overtopping a structure and an overtopping bore on the promenade overtopping a storm wall.

Analyzing the data of two model studies on crest modifications under a variety of hydrodynamic conditions provided a further discussion about composite reduction factors and the influence of components of a complex superstructure such as landward storm wall end of a promenade and SWBs. Although a direct comparison of the datasets was not possible between the two model studies, the dimensionless approach showed that the composite reduction factors should consider the interdependency of components of complex geometries as the performance of SWB depends on this interdependency significantly. However, it is also important to consider the influence of components on the composite reduction factors as seen in the influence of storm wall height in the case of the storm wall at the end of a promenade.

It is very important to carry out further research on the reduction effect of crest modifications for vertical structures (plain and composite) considering different geometries of the elements such as wall height, parapet geometry, promenade width, and slope, and other SWB configurations to determine generalized reduction factors for each element. Still, it is expected that the performance of similar modifications to the model studies in this paper will be similar for the range of hydraulic conditions tested in the study.

CRediT authorship contribution statement

Dogan Kisacik: Conceptualization, Methodology, Software, Data curation, Writing – original draft. **Gulizar Ozyurt Tarakcioglu:** Writing – original draft, Visualization. **Lorenzo Cappietti:** Data curation, Writing – review and editing.

Declaration of competing interest

The authors declare that they have no known competing financial interests or personal relationships that could have appeared to influence the work reported in this paper.

Acknowledgments

Part of this project is funded by Middle East Technical University (Turkey), Scientific Research Projects Funds (METUBAP) Grant No: BAP-08-11-2015-036 and Dokuz Eylül Üniversitesi (Turkey), Scientific Research Projects Funds (DEU-BAP) Grant No: 2016. KB.FEN.014.

References

Cappietti, L., Aminti, P.L., 2012. Laboratory investigation on the effectiveness of an overspill basin in reducing wave overtopping on marina breakwaters. Coastal Engineering Proceedings 1 (33), 20. https://doi.org/10.9753/icce.v33.structures.20 structures.

Crema, I., Cappietti, L., Aminti, P.L., 2009. Laboratory measurements of wave overtopping at plain vertical wall breakwaters in presence of an overspill stilling basin, 2009. In: Proceedings of the 4th International Short Conference/Course on Applied Coastal Research, Barcelona (SP), pp. 353–360.

Den Heijer, F., 1998. Golfoverslag en krachten op verticale waterkeringsconstructies. rapport H2014,, WLDelft.

EurOtop, 2018. In: Manual on Wave Overtopping of Sea Defenses and Related Structures, an Overtopping Manual Largely Based on European Research, but for Worldwide Application, second ed. 2018. http://www.overtopping-manual.com/

Franco, L., de Gerloni, M., Van der Meer, J.W., 1994. Wave overtopping on vertical and composite breakwaters. In: Proc., 24th Int. Conf. On Coastal Engineering. ASCE, Reston, VA, pp. 1030–1045.

Geeraerts, J., De Rouck, J., Beels, C., Gysens, S., De Wolf, P., 2006. Reduction of wave overtopping at seadikes: stilling wave basin (SWB). In: Coastal Engineering, pp. 4680–4691. https://doi.org/10.1142/9789812709554_0392.

Goda, Y., 1985. Random seas and design of maritime structures. University of Tokyo Press.

Kisacik, D., Tarakcioglu, G.O., Baykal, C., 2019. Stilling wave basins for overtopping reduction at an urban vertical seawall – the Kordon seawall at Izmir. Ocean Eng. 185, 82–99. https://doi.org/10.1016/j.oceaneng.2019.05.033. ISSN 0029-8018.

Kortenhaus, A., Haupt, R., Oumeraci, H., 2002. Design aspects of vertical walls with steep foreland slopes. In: Breakwaters, Coastal Structures, and Coastlines.

Mansard, E.P.D., Funke, E.R., 1980. The measurement of incident and reflected spectra using a least squares method. In: Proceedings of 17th International Conference on Coastal Engineering. ICCE 1980, ASCE, pp. 154–172.

Martinelli, L., Ruol, P., Volpato, M., Favaretto, C., Castellino, M., De Girolamo, P., Franco, L., Romano, A., Sammarco, P., 2018. Experimental investigation on non-breaking wave forces and overtopping at the recurved parapets of vertical breakwaters. Coast Eng. 141, 52–67. https://doi.org/10.1016/j.coastaleng.2018.08.017.

Neumann, B., Vafeidis, A.T., Zimmermann, J., Nicholls, R.J., 2015. Future coastal population growth and exposure to sea-level rise and coastal flooding—a global assessment. PLoS One 10 (3), e0118571. https://doi.org/10.1371/journal.pone.0118571. PMID: 25760037.

Pearson, J., Bruce, T., Allsop, N.W.H., Kortenhaus, A., Van der Meer, J.W., 2004. Effectiveness of Recurve Wave Walls in Reducing Wave Overtopping on Seawalls and Breakwaters. Proc. ICCE, ASCE, pp. 4404–4416.

The EU floods directive. https://ec.europa.eu/environment/water/flood_risk/, 2020.

The United Nations Office for Disaster Risk Reduction, 2020. UNDRR. https://www.undrr.org/.

Tuan, T.Q., 2013. Influence of low sea-dike crown-walls on wave overtopping discharge. Coast Eng. J. 55, 1350013. https://doi.org/10.1142/S0578563413500137.

Van Doorslaer, K., De Rouck, J., Gysens, S., 2009. Reduction of wave overtopping: from research to practice. In: 4th SCACR International Short Conference on Applied Coastal Research.

Van Doorslaer, K., De Rouck, J., Bodere, T., Vanhouwe, G., Troch, P., 2010. The influence of a berm and a vertical wall above SWL on the reduction of wave overtopping. In: Proceedings on the Third International Conference on the Application of Physical Modelling to Port and Coastal Protection. Coastlab. https://doi.org/10.13140/2.1.1008.4167.

Van Doorslaer, K., De Rouck, J., 2010. Reduction of wave overtopping on a smooth dike by means of a parapet. Coast Eng. 1–15. https://doi.org/10.9753/icce.v32.structures.6.

Van Doorslaer, K., De Rouck, J., Audenaert, S., Duquet, V., 2015. Crest modifications to reduce wave overtopping of non-breaking waves over a smooth dike slope. Coast. Eng. 101, 69–88. https://doi.org/10.1016/j.coastaleng.2015.02.004.

Zanuttigh, B., Formentin, S.M., 2018. Reduction of the wave overtopping discharge at dikes in presence of crown walls with bullnoses. Coastal Engineering Proceedings 1 (36), 110. https://doi.org/10.9753/icce.v36.papers.110.

Zerbini, S., Raicich, F., Maria Prati, C., Bruni, S., Del Conte, S., Errico, M., Santi, E., 2017. Sea-level change in the Northern Mediterranean Sea from long-period tide gauge time series. Earth Sci. Rev. 167, 72–87. https://doi.org/10.1016/j.earscirev.2017.02.009, 2017.